OPTIMAL COORDINATION OF DISTRIBUTED ENERGY RESOURCES IN ISOLATED POWER SYSTEMS: A CROSS-TIME SCALE PERSPECTIVE

A Dissertation

by

EBONY TENILLE MAYHORN

Submitted to the Office of Graduate and Professional Studies of
Texas A&M University
in partial fulfillment of the requirements for the degree of

DOCTOR OF PHILOSOPHY

Chair of Committee,	Le Xie
Co-Chair of Committee,	Karen Butler-Purry
Committee Members,	Sergiy Butenko
	Jose Silva-Martinez
	Karanjit Kalsi
Head of Department,	Miroslav M. Begovic

August 2015

Major Subject: Electrical Engineering

ABSTRACT

This dissertation investigates the problem of optimally coordinating distributed energy resources (DERs) in isolated power systems. It is motivated by the recent efforts worldwide of integrating large amounts of renewable generation into power grids to provide more sustainable electricity services. The increased penetration of renewable generation presents challenges for power systems operations due to increased variability and uncertainty occurring at multiple time scales. The challenge of coordinating resources cost effectively while ensuring adequate technical performance is even more pronounced in isolated power systems that are vulnerable to disturbances because of low inertia and limited generation capacity. Tertiary control approaches have been proposed for managing resources economically and all approaches assume time scale separation exists with lower level secondary and/or primary controls. Some works have mentioned that tertiary controls should be executed faster (i.e., seconds). However, if tertiary controls are executed faster, so as to interact with lower level control actions, this could cause exacerbated technical performance (e.g., frequency performance). The effect of dispatching at shorter time scales, on technical performance, has not yet been investigated.

In this work, such cross-coupling among different time scales is considered, and an optimal coordination (OC) strategy for isolated microgrid systems with a mix of DERs is proposed. The goals of the OC strategy are to simultaneously minimize operating costs of diesel generators and maximize the utilization of wind generation,

while considering equipment life of DERs, physical limitations on the individual controllable resources and maintain adequate frequency performance. Time scale coupling between the OC strategy and primary controls was investigated along with key parameters affecting tertiary control performance.

The effectiveness of the OC strategy is evaluated in terms of frequency, economic and computational performance under realistic scenarios. To capture the impact on frequency performance, simulations were performed on a dynamical model of an isolated microgrid system. Results suggest that the proposed approach is generalizable towards designing multi-time scale optimal coordination strategies for isolated power systems to satisfy both economic and operational objectives. Recommendations are given on extending the approach to other types of isolated power systems with different variability and uncertainty characteristics.

DEDICATION

This dissertation is dedicated to an environment that is sustainable for current and future generations. This accomplishment is dedicated to the person I have become today, after persevering through the challenging times, and to others who are traveling a road less traveled.

ACKNOWLEDGEMENTS

This PhD work was sponsored by Texas A&M University Diversity fellowship and the NACME Alfred P. Sloan Minority PhD Program. I am very grateful for these sources of funding and am happy that I am able to honor my commitment to complete my degree requirements. In addition, I would like to express deep gratitude for the people in my life who have guided, supported, encouraged and assisted me throughout my PhD work.

I would first like to thank my major advisor, Dr. Le Xie, for committing his valuable time to guiding me through to the end. I would like to extend a special thanks to my co-chair, Dr. Karen Butler-Purry for helping me to find financial support to fund my entire graduate education in addition to her dedication, advice and feedback. I am also appreciative of my other committee members Dr. Sergiy Butenko and Dr. Jose Silva-Martinez.

I am truly grateful and indebted to many of my colleagues at Pacific Northwest National Laboratory who offered their time, advice, expertise and encouragement. In particular, I would like to thank Karanjit Kalsi, Marcelo Elizondo, Jianming Lian, Frank Tuffner, Jason Fuller, and Yannan Sun.

Because the PhD process usually requires great focus and limited leisure time, I am truly thankful for the great friends and family who understood my situation and continued to support, encourage and help me find the energy to persevere through the challenging times. Without all of the great people as a part of my life before and the ones

who entered my life at the right time during this PhD process, this accomplishment may not have been possible.

TABLE OF CONTENTS

Page

LIST OF FIGURES

Page

LIST OF TABLES

Page

1. INTRODUCTION

1.1 Motivation

The generation capacity in an interconnected power system is large relative to load demand due to immense generation support from multiple areas, and the transmission system plays an essential role in supplying power from generators to loads and between interconnected areas. In contrast, an isolated power system is relatively small and may have weak or no connections with neighboring power systems. Some examples of isolated power systems include microgrids operating in islanded or isolated mode, shipboard power systems, and off-shore oil platforms [1-7]. This work is motivated by the global efforts of deploying many renewable resources in electric energy systems. However, integrating large amounts of stochastic renewable generation into power systems can introduce variations at multiple time scales, which can be seen as relatively large disturbances in isolated systems due to low inertial support. These variations can cause operational issues. Hence, there is need to rethink isolated power system operations in terms of control and coordination. Operational issues associated with integrating large amounts of renewables and isolated power system operations are discussed in the following subsections.

1.1.1 Operational issues for isolated power systems

Disturbances tend to cause vulnerability in isolated systems with relatively low inertia, which can threaten security as frequency and voltage deviate significantly. As variable and uncertain renewable penetration increases, the impact of these disturbances

can be exacerbated if not handled properly. Renewable wind generation is of focus in this work. Issues associated with high penetration of wind generation, variability in wind and load disturbances, and uncertainty due to pre-specified contingencies (e.g., loss of generator) and wind power and load forecasts are explained next.

An important issue for power system operations is high penetration levels of renewable energy resources. Penetration level can be defined in terms of instantaneous or average penetration levels [8]. Instantaneous penetration level is the ratio of power of renewable resources (wind, solar, hydro etc.) to the total load in the system. Average penetration level is the ratio of the energy of renewable resources to the energy demand of the system. Depending on the penetration levels of renewable resources the system can be considered to be low (<20% average, <50% instantaneous), medium (20-50% average, 50-100% instantaneous) and high (50-150% average, 100-140% instantaneous) as given in [8]. If a system has the capability to produce more wind power than is needed by the load, provisions such as energy storage, dump load, wind curtailment, and/or optional/deferrable loads may be used to smooth out fluctuations in the wind energy so that surplus wind does not cause frequency stability issues. A system with these types of provisions can be classified as a high penetration system.

Diesel generators are inefficient when operating at low power output levels and are usually expensive to operate due to fuel costs [9]. In a system with high penetration of wind generation and diesel generators, the diesel units can often supply the majority of the load at low wind speed. However, at high wind speeds, diesel generators will have to either operate at the minimum loading recommended by the manufacturer or shut off

to allow the wind generation to pick up the entire load in the cases when there is a surplus of wind generation [9-11].

Variability in wind and load can impact the ability maintain balance between generation and loads or acceptable frequency and voltage profiles [9, 12] in power systems. For this reason, it is important to understand the characteristics of load/wind variability when determining the contributions of each DER to meet the load demand.

In isolated power systems, load changes can be more significant compared to interconnected systems, depending on the types of loads being served and whether the system has relatively low inertia. However, loads typically follow diurnal patterns that are fairly predictable. An example of a daily load patterns for a residential area with ~1000 homes in Northeastern Oregon during Fall of 2011, is given in Fig. 1. The middle line (green) represents the average load demand. The upper (blue) and lower (red) lines represent the maximum and minimum load demand, respectively. These day to day variations of the load demand are relatively predictable within the minimum and maximum load bands.

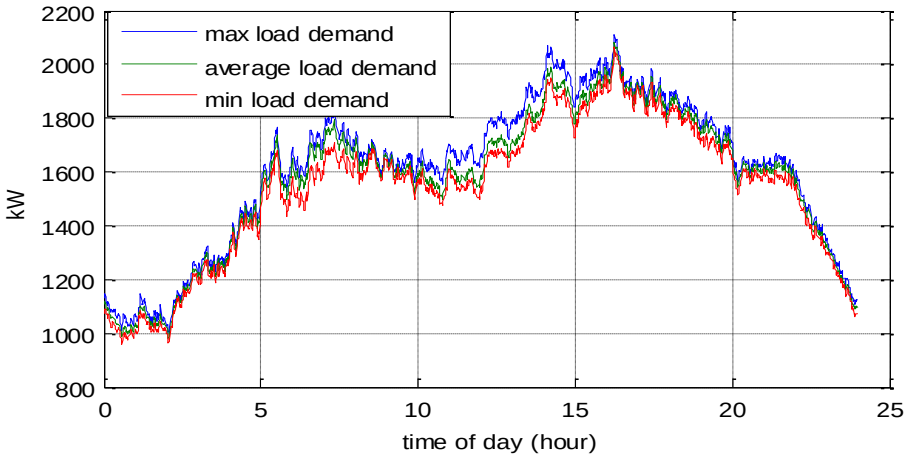

Fig. 1 Daily load pattern for a residential area

The additional wind power variations typically impact power system operations on various time scales as described in [9, 11, 13]. This variability can exacerbate challenges with balancing generation and load in the short- and long-term in high wind penetration systems. An example of wind power versus load variations that could occur in an isolated power system with high wind penetration, over a 4 hour period, is shown in Fig. 2. In this particular case, the minute by minute variations in load and wind are ±60 kW and ±600 kW, respectively. In addition, the hourly variations in load are fairly constant, but the wind generation varies by 1600 kW over a 2 hour period. These variations in wind and load result in the netload (load minus wind power) profile, displayed in Fig. 3, which is much more volatile in both the minute and hourly time frames, compared to the normal load demand changes shown in Fig. 2.

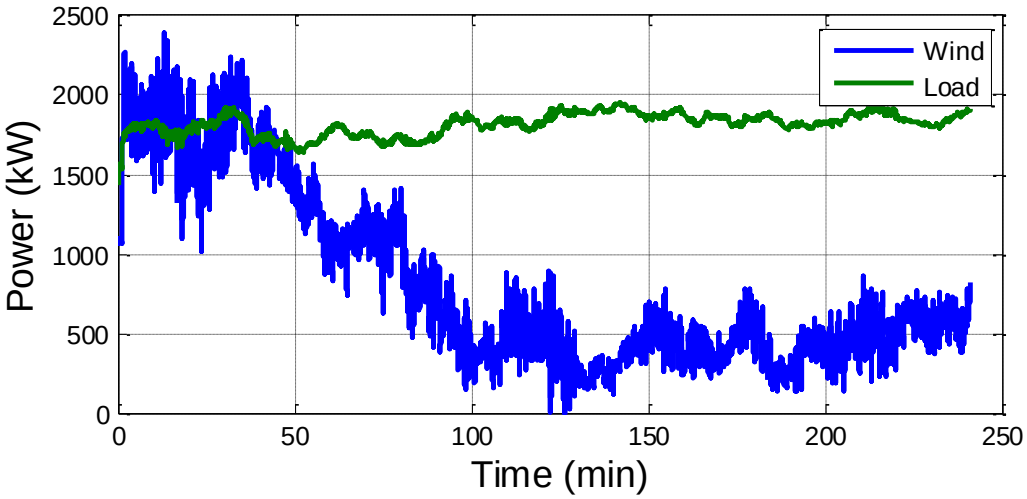

Fig. 2 Wind power and load demand for high wind penetration example

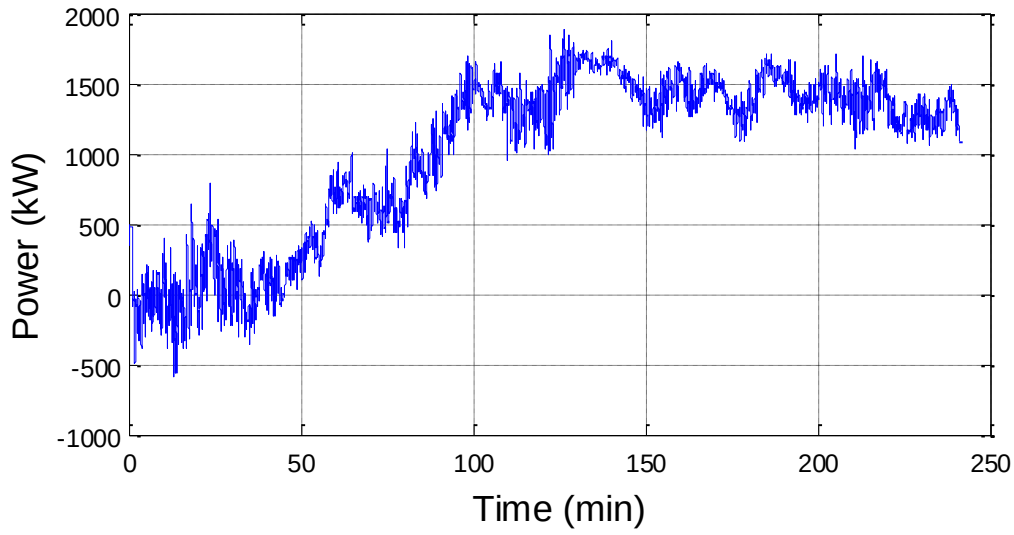

Fig. 3 Netload for high wind penetration example

Significant variability from load and wind may cause undesirable cycling in battery energy storage as these devices will need to charge and discharge frequently to

help compensate for the variability. Also, if not coordinated properly, diesel generators would have to cycle (start and stop) frequently, which could degrade the life of the diesel generators [14-16].

With increased uncertainty due to wind forecasts added to uncertainty in load forecasts and pre-specified contingencies, balancing power becomes more challenging in isolated power systems. This uncertainty in load and wind forecasts, as well as pre-specified contingencies poses concerns for system security in isolated power systems. The main concern for security is frequency stability because it depends on the ability to maintain balance between system generation and loads, without unintentional loss of load. Instability that may occur is usually as result of sustained frequency swings that cause generators or loads to trip [17]. Issues with frequency stability are commonly related to equipment lacking capability to respond in a timely fashion, poor coordination of controls and protection, or insufficient generation reserve [17]. Frequency stability is especially of concern in isolated power systems where responses to disturbances can cause relatively significant loss of load or generation.

To safeguard against frequency instability, it is important to have accurate forecasts of wind and load. In particular the wind forecast error increases as the forecast horizons increases [9, 11, 18-20]. Hence, short-term forecasts of wind power and load demand should be considered as discussed in [13, 18, 20]. Also, coordination decisions for controllable resources should be made with consideration of maintaining adequate reserves across available resources to handle system uncertainties. The reserves should be distributed in a way that will allow resources to share the responsibility of responding

to differences in forecasted and actual wind and load, as well as a large contingency without load shedding [21-24].

1.1.2 Isolated power system operations

Isolated power system operations as discussed in [25] is typically divided into several hierarchical control layers to maintain economic, reliable and secure operation over multiple time scales. Specifically, the different levels of control include primary, secondary (e.g., automatic generation control (AGC)), and tertiary (e.g., economic dispatch (ED) and unit commitment (UC)).

Primary frequency controls are local, automated controls at device or resource level that are used to arrest and stabilize frequency following disturbances. Primary controls typically occur within the time scale of milliseconds to seconds. Inverter-based and power sharing controls are the two most commonly used primary control approaches for microgrids. Inverter-based control typically consists of an outer- and inner- loop for voltage control and current regulation, respectively [25]. Power sharing involves using active power-frequency and reactive power-voltage PI-controllers to emulate the droop characteristics of synchronous generators [25]. An extensive review of additional primary control approaches can be found in [25].

Secondary frequency control occurs on the time scale of seconds to minutes. This type of control is centrally coordinated, yet automated to balance generation and load by restoring frequency and voltage to their nominal values. Examples include real-time load management and automatic generation control (AGC).

Tertiary controls are centralized controls that are used to optimally dispatch and commit resources according to system operational objectives. Examples of tertiary controls include economic dispatch (ED), volt-VAR control, and unit commitment (UC). These controls are typically are executed in the time scale of minutes to hours.

In order to remedy operational issues that may be caused by increased renewable generation in isolated power systems, such as, isolated microgrids; there is a need for enhanced controls at all levels of operation. For example, tertiary control approaches for reactive power coordination and voltage control have been proposed for isolated microgrids and shipboard power systems in [26, 27]. In addition, faster execution of tertiary controls should be considered to follow the increased variation introduced by renewable generation. When enhancing in control functions at different levels and executing controls faster, coordination should still be maintained between the control layers. The focus of this work is on developing an optimal coordination strategy, which includes enhancing the ED tertiary control function to coordinate DERs in isolated power systems and maintaining coordinating with lower level controls (e.g., primary controls) so that adequate frequency control performance can be maintained.

1.2 Class of isolated power systems

The class of isolated power systems studied in this work is microgrids operating in islanded mode with less than 100 MW of peak load. Many issues increasingly threaten security, reliability, and quality of conventional electric power systems (EPSs): aging transmission/distribution infrastructure, growth in load demand, additional stresses due to deregulation, the integration of non-traditional generation (i.e., wind, solar, fuel cell,

etc.) [28]. The microgrid concept was introduced to circumvent social and practical limitations associated with the macrogrid expansion, a solution typically used to address the aforementioned issues.

Microgrids can be distribution networks that make use of distributed energy resources (DERs) that are co-located near the loads to supply local demand [28]. Components of the microgrid consist of distributed energy resources (DERs), interconnection switches, and control systems [4]. DERs are small scale power generation technologies, typically rated between 3kW and 10MW, which are used to provide an alternative to conventional EPS. DERs can be further classified as either distributed generation (DG) or distributed storage (DS) units. DGs are sources of energy; for instance: microturbines, fuel cells, wind turbines, PV arrays, reciprocating internal combustion engines with generator, etc. DSs are storage devices, such as, batteries, supercapacitors, and flywheels. A microgrid is typically operated in 3 different modes [29]:

- Isolated grid (IG) –DERs supply all power to meet local load without support from a macrogrid (autonomous mode)
- Grid-independent (GI) – DERs provide baseload power to all local loads and the main grid provides back-up power when needed
- Grid-dependent (GD) – main grid provides power to all local loads and DERs provide back-up power when needed.

An interconnection switch is a point of common connection (PCC) between the microgrid and the larger interconnected grid [4]. Measurements are taken on both sides

of a PCC for determining system operating conditions, and the location of the PCC determines whether a microgrid is a utility, multi-facility/single facility, or remote microgrid [4]. A typical representation of a distribution microgrid is shown in Fig. 4 .

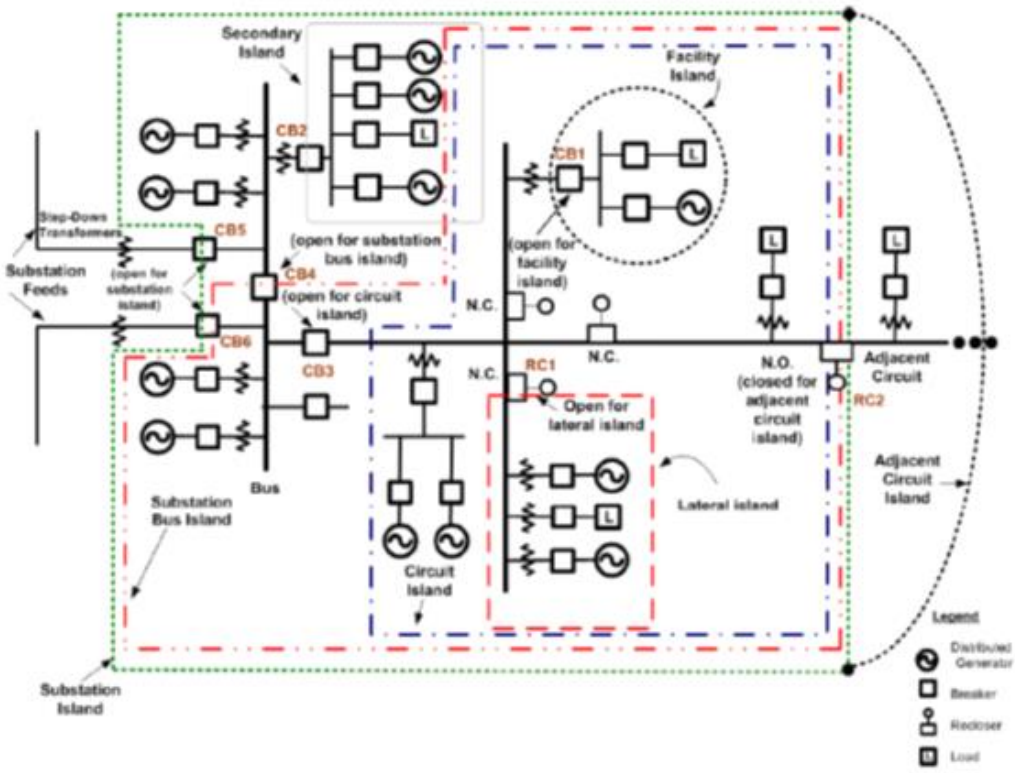

Fig. 4 An example of an islanded distribution microgrid configuration (reprinted with permission from [12] © 2011 IEEE)

If the PCC is located at the substation feeders, it is called a utility microgrid. A utility microgrid is typically composed of a portion of or all distribution substation feeders that can be managed by a distribution network operator (DNO). This microgrid type has the potential to accommodate local load growth, manage congestion on distribution feeders

and sub-transmission networks, and provide ancillary services for local supply of reactive power and premium power quality [30]. Within the class of utility microgrids, three island configurations are possible. As shown in Fig. 4, these islands can be identified by the following [12]:

- Substation bus island – island designed to allow only a single bus within a substation to serve loads, although multiple buses may be used. This is demonstrated by the outer red dashed line in Fig. 4. This island type is typically intended for situations where a substation feed or substation transformer is out of service.
- Substation island – island formed to allow a single substation to supply the load as shown with the green dashed line in Fig. 4. This island may be formed when an entire distribution substation is out of service or when one substation transformer is out of service and the other transformer incapable of supplying the entire substation load. This type of island is also beneficial for purposes of lessening thermal overload and voltage problems on the substation feeds or overload problems on substation transformers.
- Adjacent circuit island – island formed to supply load in a main and adjacent circuit if there is a loss of the adjacent circuit feed, along with the main substation feed as shown by the black dotted line in Fig. 4.

Similarly, if the PCC is connected within the distribution grid to serve one or multiple facilities, it is considered a single/multi-facility microgrid. These types of microgrids can supply load in commercial/industrial complexes that tend to be sensitive and critical

loads that require a high degree of power quality and reliability. Some examples include: a university campus, a shopping center, and an industrial center [4]. These microgrids can also be setup set up to serve a small multi-facility residential customer, such as a group of townhouses and suburban areas. There are two possible configurations for single-facility microgrids as shown in Fig. 4, which are identified as follows [12]:

- Lateral island – island is designed to serve load on a lateral on a distribution circuit when a switching device (e.g., the breaker, recloser, or sectionalizer) opens.
- Facility island – island formed with only one PCC (CB1) with the main grid to allow generation to serve the load of a customer facility.

For multi-facility microgrids, there can also be two types of island configurations as shown in Fig. 4, which are distinguished as follows:

- Circuit island – island formed to serve the load on a single distribution circuit or feeder when there is a loss of the substation feed, transformer, or bus.
- Secondary island – island formed on the secondary side of a distribution transformer where one or more DER serve multiple customers.

If there is no PCC anywhere between the main grid and microgrid, the microgrid is considered remote. Remote microgrids, of course, have only one operating mode. A remote microgrid is typically designed to enable the DERs to supply the entire load in addition to maintaining an appropriate level of reserve capacity for contingencies that may occur in the system [30].

Microgrid testbeds have been developed in different geographic locations such as in the United States, Japan, Canada, and Europe [4]. The set-up and operation of the test sites vary from case to case. For example, the US CERTS microgrid in the US does not have renewable energy sources included in its architecture [31]. Also, the Europe Microgrid projects include a couple of test sites with different topologies [32]. A review of microgrids, developed in different regions across North America, Europe and Asia, is given in [33].

1.3 Review of existing economic dispatch approaches

There have been several ED approaches proposed for grid-connected microgrids and large scale interconnected systems to handle increased penetration of renewable generation, as described in [34-39]. Since the OC strategy is an enhanced ED function and ED theory is well established in the literature for grid-connected microgrids and interconnected power system, a review of different dispatch and coordination strategies for isolated systems will be presented in section 1.3.1. In section 1.3.2, research gaps are identified in terms of the ability of existing ED approaches to address operational challenges introduced by integrating large amounts of renewables in isolated power systems. These research gaps highlight the need for an adequate OC strategy for microgrid systems operating in isolated mode with high wind penetration.

1.3.1 Economic dispatch approaches for isolated power systems

Isolated systems are typically managed conservatively by maintaining large amounts of operating reserves. Higher costs are often a result of operating in a

conservative way, which can outweigh the expected benefits of utilizing additional renewable generation resources within these systems. For this reason, it is desirable to also consider economics of operating the resources when managing power in isolated microgrids in addition to security and reliability. A few approaches for ED have recently been proposed for isolated systems including microgrids. These works were motivated by the need to develop novel optimal coordination strategies to mitigate some concerns for relatively low inertia systems with increased variability and uncertainty due to intermittency of renewable generation. Some of these strategies will be reviewed next.

A conceptual design of a centralized energy management system (CEMS) architecture was presented in [40] for microgrids in the isolated mode that may contain any of the following DER types: thermal storage, fuel cells, wind turbines, photovoltaic solar arrays, microturbine combined heat and power (CHP) units, fuel cell electrolyzer energy storage. A receding horizon optimization method was recommended for the class of solution methods to be used to solve the multi-stage ED that was also introduced within the CEMS architecture, as shown in Fig. 5. In receding horizon optimization, a finite horizon optimization problem is solved at each time step, where the output is a control sequence for the given prediction horizon. Only the first control step of the sequence is implemented, and the process is then repeated after receiving feedback system states. The optimization horizon was recommended to be a few minutes to hours.

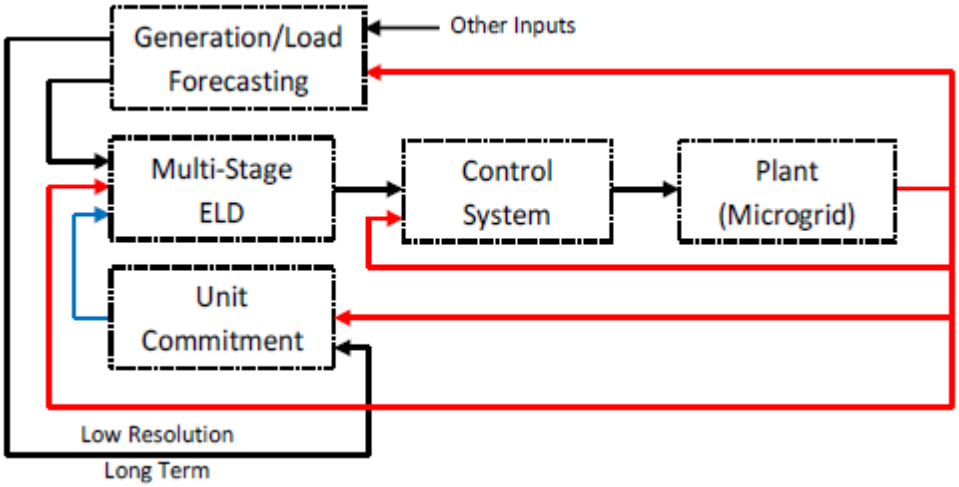

Fig. 5 CEMS conceptual architecture (reprinted with permission from [40] © 2011 IEEE)

Another specific isolated system that uses the CEMS structure is the Crete system [41], which is the largest Greek island system with above 400 MW of peak load and 60 MW of installed wind generation capacity. The CEMS was developed to target the needs of medium and large-scale isolated systems with high penetration of renewables (>20%), comprising of steam and diesel or gas units. The hierarchical structure of the CEMS used for the Crete system is shown in Fig. 6. The load and renewable forecasting, unit commitment (UC), economic dispatch (ED), and security monitoring and assessment modules are common within a CEMS. The objective of the ED module was to minimize cost of operations subject to power balance, bus voltage, and reactive power generation constraints, along with constraints for bilateral contracts with independent power producers (IPPs) of renewable power. Dispatch decisions were made every 20 min.

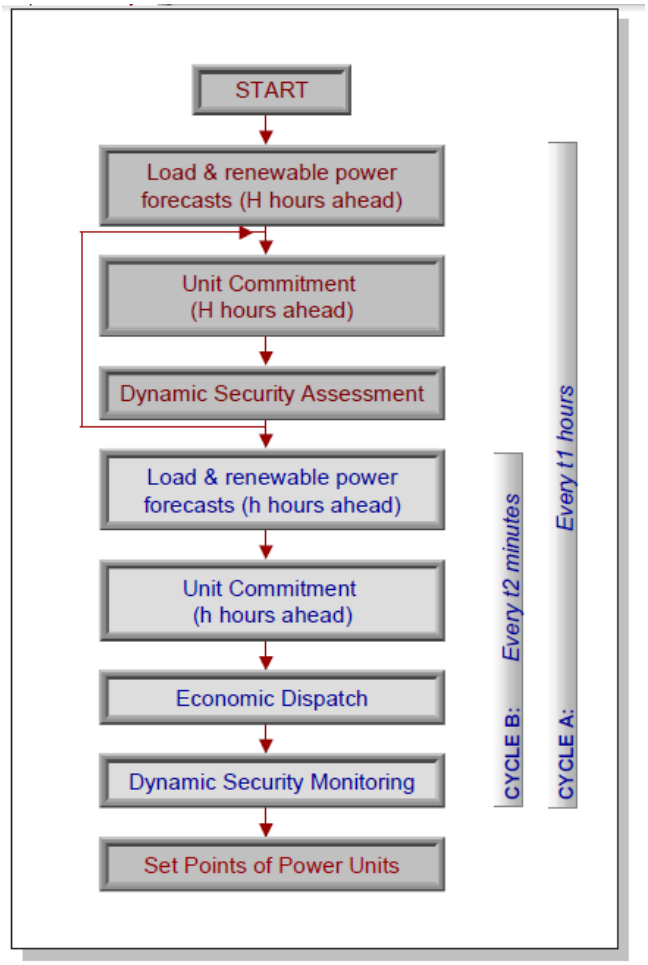

Fig. 6 CEMS architecture for the Crete system (reprinted with permission from [41] © 2002 IEEE)

In [22], a constrained static economic dispatch (SED) approach was proposed to coordinate the dispatchable wind and thermal generation in an isolated power system through reserve. The reserve constraints were used as a precaution for large contingences and unpredictable wind and load variations that threaten system security. The feasibility and effectiveness of the approach was studied based on a static model of the Taiwan

Power System, which is a 345 kV transmission network with 52 thermal generating units, 0 to 6000 MW of wind capacity, and a peak load of 19000 MW.

In [42], an economic dispatch formulation and solution method was developed to provide optimal power references to controllable DGs such as diesel generators in a multi-area microgrid in the grid-connected mode. Non-controllable DGs such as wind and solar generation sources are treated as negative loads. The basic static ED formulation is used in [42] with the addition of the following reserve constraints for security purposes: 1) reserve requirements to compensate uncertainty in the power output of renewable resources, 2) flow restrictions between control areas, and 3) reserve requirements for the stable operation during the islanded mode. DSM was also used as the solution method for the static optimization problem formulation. The Taiwan power system with 10 diesel units was also used to illustrate the effectiveness of the method. However, the load was scaled down to a 2200 MW peak load and a 2625 MW diesel generator capacity.

1.3.2 Research gaps for existing economic dispatch approaches

The research presented in this dissertation addresses the problems related to coordinating diesel, wind and energy storage resources, optimally, in a low inertia, microgrid operating in the isolated mode. Several research gaps, in the ability of the methods discussed in 1.3.1 to address the operational issues introduced in isolated power systems by high penetration of renewables, have been identified and are summarized here.

- The proposed ED approaches do not verify sufficiency of a comprehensive strategy in terms of overall problem formulation and solution method. Based on the operational issues introduced by renewables, the proposed approaches should have the essential components necessary to coordinate the DERs to simultaneously minimize operating costs, maximize the utilization of renewables while considering the life and efficient utilization of resources and ensuring adequate system frequency performance. Many of the approaches consider objectives and constraints in the formulation to meet most goals simultaneously, but do not consider elements in the formulation that will limit the impact of the renewable generation on the life and efficient utilization of non-renewable generation resources. Also, all ED approaches fundamentally assume time scale separation and employ a steady state power balance constraint to maintain adequate frequency performance. In conventional bulk power systems, time scale separation can be well justified from singular perturbation theory [43]. However, increased variations at multiple time scales may render such an assumption to be invalid in isolated power systems. This means that the steady state power balance traditionally employed to maintain adequate frequency performance may not be adequate. The validity of the steady state power balance constraint has not been investigated for high wind penetration cases. Furthermore, the approaches do not consider all important characteristics that are necessary to compensate for increased variability and uncertainty introduced by renewables. Model predictive control (MPC) has been identified and demonstrated to be an effective solution

method for interconnected power systems and grid-connected microgrids [25] because of its look-ahead capability to foresee how present decision can influence response capability of the dispatchable DERs at a future time. In addition, MPC incorporates a feedback mechanism that allows for frequent updates in control decisions to compensate variability and uncertainty. However, in [25], it was questioned whether MPC is an appropriate solution method to compensate for variability and uncertainty in isolated power systems that are more vulnerable to disturbances. A conceptual multistage ED technique is presented in [40] based on MPC principles, but the approach has not been further demonstrated to be effective for isolated power systems

- In all proposed ED approaches, dispatch is executed every 5-20 minutes. It is hypothesized that faster execution should be considered to enable controllable DERs to follow the variations in wind and load disturbances in a more cost-effective manner. However, faster execution could have an impact on the coupling between ED and lower level control time scales, causing exacerbated performance of lower level controls. Time scale coupling between control levels has not been considered in any of the reviewed methods because of the execution time step chosen in addition to the time scale separation assumption.
- Steady state analysis is generally used to evaluate the effectiveness of the strategies. This causes difficulty in analyzing whether the strategy degrades system technical performance (i.e., frequency performance) in a dynamic power system. The analysis for ED approaches has not been extended to consider

dynamics in order to investigate impacts on frequency performance and coupling with lower level controls as faster execution is considered.

1.4 Contributions of this work

Based on the research gaps identified in section 1.3, the main contributions of this dissertation are as follows:

- A comprehensive optimal coordination strategy was developed, consisting of an adequate formulation, appropriate solution method and a systematic way of selecting key parameters impacting performance and coordination with lower level controls. Specifically, an online receding horizon based optimization strategy is proposed for isolated microgrid operation to handle increasing variability and uncertainty due to high penetration of renewables. The proposed strategy is simultaneously able to meet the following objectives: minimize operating costs and maximize the utilization of wind generation, while considering equipment life and physical limitations of controllable DERs, and maintaining adequate frequency performance.
- The OC analysis was extended to consider dynamics to investigate impact of tertiary frequency control performance and time scale coupling with lower level controls as faster execution of the OC strategy is considered.
- Recommendations were made for designing multi-time scale optimal coordination strategies for isolated power systems with unusually high levels of variability and uncertainty.

1.5 Dissertation organization

In this section of the dissertation, a review was presented on the characteristics, technical issues, and operations of isolated systems, along with the various optimal coordination strategies that have been proposed for conventional and isolated systems. These topics are important to understand when developing new strategies for microgrids in the isolated grid mode. The research gaps, based on the ability of the reviewed ED approaches to address operational issues identified, were summarized to highlight the need for an adequate OC strategy for high wind penetration microgrid systems operating in an isolated mode and the contributions of this work.

The remaining dissertation is organized as follows. Section 2 presents a comprehensive OC formulation for a low inertia isolated microgrid that contains a high penetration of wind generation, diesel generators and battery energy storage. Section 3 focusses on expressing the OC formulation developed in section 2 in a receding horizon optimization framework namely model predictive control. The efficacy of the MPC based optimal coordination strategy demonstrated using a dynamical model of an isolated microgrid system in section 4. In particular, a number of realistic test scenarios and performance metrics are presented, which were used to select key parameters for the proposed OC strategy and make recommendations on designing of multi-time scale OC approaches for isolated power systems.

2. MULTI-SCALE OPTIMAL COORDINATION PROBLEM FORMULATION

2.1 Introduction

As implied in section 1, there is a need to develop novel optimal coordination strategies for low inertia isolated power systems with high penetration of renewable generation. The focus of this section was to develop an optimal coordination strategy for microgrids operating in the isolated mode, consisting of high penetration of wind generation, diesel generators and energy storage. The aim of the OC strategy is to coordinate these distributed energy resources by determining optimal setpoints for the resources committed during islanded operation of the microgrid while maintaining frequency performance. Specifically, it is desired to simultaneously meet the following objectives: minimize operating costs and maximize the utilization of wind generation, while considering equipment life and physical limitations of controllable DERs, and maintaining security and adequate frequency performance.

Several assumptions were made about the isolated power system considered in this work:

- System losses are assumed to be negligible.
- Real power and frequency are decoupled from reactive power and voltage. Specifically, the power output of dispatchable DERs depends on primary frequency droop control. Voltage/reactive power control is handled by decentralized controllers (i.e., AVR exciter controls in diesel generators,

voltage regulators and capacitor switching within the network). Since voltage control was assumed to be handled by decentralized controllers and possibly separate supervisory control modules (e.g., optimal Volt-VAR control), it was not a focus of this work.

- Hierarchical control layers consist of primary and tertiary controls. As mentioned in section 1, secondary controls such as AGC are ignored.

The OC problem formulation is formulated as a dynamic optimization problem where the optimal solution depends on the trajectory of the state and control variables over a horizon. The system objectives and constraints are discussed in sections 2.2 and 2.3, respectively. The overall problem formulation is presented in section 2.4. Finally, a summary is given in section 2.5.

2.2 Objectives of the OC problem

The main objectives of the OC problem are to minimize operating costs of diesel generators and to maximize wind power use, as well as maximize life of energy storage units and diesel generators. The operating costs and wind utilization objectives were expressed in terms of soft constraints. Furthermore, objectives to maximize the life of energy storage and diesel generators were represented as hard constraints. Soft constraints are objective functions that are used to express preference for solutions. Hard constraints are referred to constraints that must be satisfied.

The operating costs of diesel generators are mainly based on fuel costs and can be represented as linear or quadratic functions as given in [44] and references therein. The cost coefficients are determined by curve-fitting based on the diesel fuel

requirements for different generation levels as given in [45]. A quadratic fuel cost function $C_j\left(P_{Gj}(k)\right)$ was used for the OC method and the overall cost is shown in (1).

$$\min_{P_G}\sum_{k=1}^{K}\sum_{j=1}^{G}C_j\left(P_{Gj}(k)\right)=\min_{P_G}\sum_{k=1}^{K}\sum_{j=1}^{G}\left(a_j+b_jP_{Gj}(k)+c_jP_{Gj}^2(k)\right)\Delta t \tag{1}$$

a_j, b_j and c_j are fuel cost coefficients of diesel generator j expressed in \$/hr., \$/kWh and \$/hr./(kW)^2, respectively; $P_{Gj}(k)$ is the power output of the *j-th* diesel generator at time step k; Δt is the time step duration in hr., G is the set of diesel generators; and K is the horizon over which the optimization is performed.

To maintain system power balance and reliability in the presence of high wind penetration, it is often necessary to curtail wind power generation. In this work, it was assumed that the wind generators are non-dispatchable and excessive generation has to be curtailed or dumped when necessary. However, curtailing the wind can be counterproductive and a large amount of curtailment can have a significant impact on wind generator economics. Therefore, to maximize wind power utilization, it is desirable to minimize the amount of wind curtailed. This objective was represented as a soft constraint in the objective function to allow curtailment only when power cannot be balanced by the diesel generators and energy storage. The cost of wind energy curtailment C_w is expressed based on the marginal cost of wind energy curtailed which is given by (2).

$$\min_{P_{curtail}(\mathrm{k})} C_w(P_{curtail}(k))=\min_{P_{curtail}(\mathrm{k})} d\sum_{\mathrm{k}=1}^{\mathrm{K}}P_{curtail}(k)\Delta t \tag{2}$$

$P_{curtail}(k)$ is the amount of wind power curtailed at time k, d is the marginal cost of wind energy curtailment, which can be determined based on production tax credit, avoided energy costs, CO2 emissions costs and/or renewable energy credit opportunity cost [46] in $/hr. The amount of wind power curtailed is defined as the total amount of wind generated minus the amount of wind that is utilized.

Therefore, the overall objective function is expressed as a combination of the cost of fuel and wind curtailment objectives in (1) and (2) can be mathematically written as J which is defined in (3).

$$\min_{P_{curtail}(k),P_{Gj}(k)} J = \sum_{k=1}^{K}\left[\sum_{j=1}^{G}\left(a_j + b_j P_{Gj}(k) + c_j P_{Gj}^2(k)\right) + dP_{curtail}(k)\right]\Delta t \tag{3}$$

2.3 System and DER operating constraints for OC problem

In addition to the objective function, important constraints or limitations should be considered, regarding the problem, to obtain a feasible solution. System and individual DER operating constraints on security, power/energy limitations, ramp rate limits, as well as system power balance are important to consider in the OC problem for high penetration levels of wind generation, variability in wind power and load demand, and uncertainty due to contingencies, and wind power and load forecasts. The selection of the mathematical representations of these constraints is discussed in the following subsections.

2.3.1 System security reserve constraints

Since it is desired to coordinate the resources to meet the system objectives in a secure way, security constraints in the form of emergency reserve requirements were determined for the OC problem. In isolated power systems, frequency instability can be mitigated by ensuring there is sufficient reserve available in the DERs and that the reserves can be deployed quickly enough following a large disturbance as mentioned in [47]. As discussed in [47], battery storage units and conventional generation units typically have response times within the ten to hundreds of milliseconds and seconds time frame, respectively. The power reserves in conventional generators cannot be deployed fast enough to prevent frequency instability in a relatively low inertia isolated grid. However, depending on the system inertia and response time of the battery storage, an adequate amount of battery storage reserves can be used to arrest system frequency within admissible limits. Therefore, the security reserve constraint, shown in (4), was chosen to allocate adequate reserves for the fast-acting battery storage units, based on the constraint proposed in [21]. The effectiveness of the constraint in maintaining frequency stability is dependent on system inertia and the response capability of the battery storage. The frequency control settings of the battery storage, such as frequency deadband setting, can impact the response capability.

$$\sum_{i=1}^{S} P_{URSi}(k) \geq \Delta P(k) \tag{4}$$

$\mathrm{P}_{URSi}(k)$ is the power reserve for the *i*-th battery energy storage unit at decision step k. $\Delta P(k)$ is the power output of the largest diesel generator, which represents a worst case

contingency, at decision step k. S is the number of battery storage units operating at decision step k.

2.3.2 Battery energy storage power and energy limits

Battery energy storage systems have power and energy limits. Based on the reserve constraints derived in (4), the upper power limit on the storage power $P_{si}^{\max}$ can be represented by the expression given in (5).

$$P_{si}(k) + P_{URSi}(k) \le P_{si}^{\max} \tag{5}$$

where $P_{si}(k)$ is the power output of the *i*-th battery energy storage unit. The sum of the power dispatched and the up reserves of the storage unit are constrained to be less than or equal to the maximum storage power output allowed. Also, the lower limit on the storage power is given by (6).

$$P_{si}^{\min} \le P_{si}(k) \tag{6}$$

$P_{si\min}$ is the minimum power limit for the *i*-th battery energy storage unit.

In order to make sure the energy limits of the battery are considered, the trajectory of the battery State-of-charge (SOC) needs to be tracked. The SOC is a temporal (dynamic) constraint. The authors in [48-50] describe how the energy remaining in the battery changes over time based on the power output. The mathematical representation of this constraint, generalized for the *i*-th storage unit, is given in (7) [48-50].

$$SOC_i(k+1) = SOC_i(k) - \alpha P_{si}(k) \tag{7}$$

$SOC_i(k)$ is the state-of-charge of the *i*-th energy storage at time step k, α is a constant given by $\alpha = \frac{\eta}{E_i^{\max}} \Delta t$ where, Δt is the time step duration (hrs.), $E_i^{\max}$ is the energy capacity of the *i*-th storage unit (kWh), and η is the efficiency of the storage unit. It is assumed that η is the same for charging and discharging of the battery unit.

To maximize the life of battery storage during operations, which is one of the OC objectives, operating limits were placed on the energy. The overall constraints on the SOC can then be mathematically represented as given in (8).

$$SOC_i^{\min} \le SOC_i(k) - \alpha P_{si}(k) \le SOC_i^{\max} \tag{8}$$

It is known that operating a battery at low SOC reduces the expected life of a battery as discussed in [48, 51]. The deep discharges in SOC that are lower than 30% should be avoided to maximize the life of battery storage [48, 51]. In (8), $SOC_i^{\min}$ is the minimum limit on the battery state of charge and should be chosen to be greater than 0.3 which prevents the battery life from drastically degrading. It should also be mentioned that this constraint causes the need for increased capacity, and in turn higher capital costs. If the battery is not allowed to go below the $SOC_i^{\min}$ value, then the life of the battery will inherently be maximized. Battery energy storage units act relatively fast compared to conventional generation. However, energy limits in (8) inherently constrain the ramping capability of these devices.

2.3.3 Diesel generator power output level

The limits on the diesel generator at each decision step k, are given in (9).

$$P_{Gj}^{\min} \le P_{Gj}(k) \le P_{Gj}^{\max} \tag{9}$$

The minimum generator power output should be selected to be at least 30% of the maximum rating of the diesel generator to minimize cycling and inefficient operation of the diesel generators [14]. This is because increasing wind penetration will cause excessive generator movement and more frequent generator cycling, causing additional stresses on equipment as stated in [15, 16]. As a consequence, the cycling generators will experience altered capacity factors and higher operational costs [15]. Constraining the minimum power output of the diesel generators helps to consider generator life during operation which could be degraded when there is a high penetration of renewable generation. The ramp limits on the diesel generators can be represented by (10), as given in [44] and references therein.

$$\left|P_{Gj}(k+1) - P_{Gj}(k)\right| \le R_{Gj}^{\max} \tag{10}$$

$R_{Gj}^{\max}$ is the maximum allowed power change of the j-th diesel generator from one time step to the next.

2.3.4 Wind generator curtailment limits

Even though wind generation is not controllable, it is necessary to curtail wind generation power output when there is excess wind generation in the system. The amount of wind power curtailed should not be greater than the amount of wind power that can be produced at any time. Therefore, a constraint on the amount of wind power that can be curtailed is given by (11).

$$0 \le P_{curtail}(k) \le P_{curtail}^{\max}(k) \tag{11}$$

$P_{curtail}^{\max}(k)$ is the maximum wind curtailed at each decision step and should be equivalent to the amount of wind generation forecasted for that time step.

2.3.5 Power balance

It is also necessary to maintain power balance to ensure that the power to be dispatched (solution) equals the power demanded by the network which is the total losses plus load power demand [52-55]. For the OC problem, the power balance equation can be represented by the expression given in (12).

$$\sum_{i=1}^{S} P_{si}(k) + \sum_{j=1}^{G} P_{Gj}(k) - P_{curtail}(k) = P_L(k) - P_w(k) \tag{12}$$

$P_w(k)$ is the total power generated by the wind generators and $P_L(k)$ is the total load in the system at time step k. In most of the previous work, large dispatch time steps are assumed and hence that multi-time scale coordination exists. However, due to the increased variability and uncertainty in isolated systems, it may become necessary to dispatch faster. This means that the power balance constraint may not be adequate for ensuring frequency performance if steady-state assumptions do not hold true. The conditions under which the power balance equation is adequate are given by:

- Condition 1: Netload forecasts are accurate so that storage and diesel setpoints can be selected to match netload
- Condition 2: Primary controls have stabilized system dynamics to steady state and that disturbances in wind and load are not significant between OC time steps

The derivation of the above conditions are based on the derivation presented in [56]. Condition 1 implies that a solution method for the optimal coordination strategy needs to be selected to compensate for variability and uncertainty inherent in net load forecasts. Condition 2 implies that the time step of the OC strategy needs to be selected carefully.

2.4 Overall formulation of OC problem

The OC formulation presented in sections 2.2 and 2.3, is adequate for isolated systems with high penetration of wind generation because it considers the issues related to the following: 1) significant variability in wind and load by considering equipment life given in (8) and (9), as well as the ramping capabilities of individual resources in (5), (6), (8) and (10); 2) security in terms of uncertainty due to large contingencies and forecast error in load and wind by ensuring adequate reserves of system and individual DERs given in (4); 3) high penetration of wind power by limiting diesel units to operate at recommended output and by minimizing the amount of wind power curtailed as given in (2). The formulation also includes basic system operating constraints on power balance in (12), as well as limitations of power, energy and ramping of individual DER resources.

The final mathematical representation of the OC problem is given in (13) and is shown in the standard form of a dynamic optimization problem.

minimize

$$J = \sum_{n=0}^{N-1} \sum_{j=1}^{G} \left[a_j + b_j P_{Gj}(n) + c_j P_{Gj}^2(n) + dP_{curtail}(n)\Delta t \right]$$

subject to

$$\begin{aligned}
& SOC_i(n+1) = SOC_i(n) - \alpha P_{si}(n) \\
& P_{si}(n) + P_{URSi} \le P_{si}^{\max} \\
& -(P_{si}(n) + P_{URSi}) \le -P_{si}^{\min} \\
& SOC_i(n) \le 1 \\
& -SOC_i(n) \le -SOC_i^{\min} \\
& P_{Gj}(n) \le P_{Gj}^{\max} \\
& -P_{Gj}(n) \le -P_{Gj}^{\min} \\
& \left| P_{Gj}(n+1) - P_{Gj}(n) \right| \le R_{Gj}^{\max} \\
& P_{curtail}(n) - P_w(n) \le 0 \\
& -P_{curtail}(n) \le 0 \\
& -\sum_{i=1}^{S} P_{URSi}(n) \le -P_{UR}^{\min} \\
& \sum_{i=1}^{S} P_{si}(n) + P_w(n) + \sum_{j=1}^{G} P_{Gj}(n) - P_{curtail}(n) - P_L(n) = 0
\end{aligned} \tag{13}$$

Dynamic optimization is obtaining an optimal solution over a time horizon where the connections between previous, current and future times are considered. The optimal solution depends on a complete trajectory of the state and/or control variables over time. These problems are setup to minimize or maximize an objective functional by determining the control trajectory while subject to 1) dynamic constraints on each state variables that model how the control variables drive the state variables over time and 2) other possible constraint types such as inequality and equality constraints. The state

variables for the OC problem are SOC_i. The control variables are considered to be the P_{Gj}, P_{si}, P_{URSi}, and $P_{curtail}$. Also, $P_L(k)$ and $P_w(k)$ represent the disturbance variables.

2.5 Summary

A formulation for the OC problem was presented based on the problem statement in section 2.1. The goals of the optimization problem are to minimize operating costs and to maximize the utilization of wind power while considering equipment life of generators and energy storage. Also, physical limitations on the individual controllable resources (i.e., generation limits, storage energy limits, etc.) were considered, as well as system operating constraints designed to maintain system security. The issues associated with variability in wind power and load demand, uncertainty due to contingencies and wind power and load forecasts, and high penetration levels of renewables were considered when formulating the optimization problem by including the appropriate objectives and constraints. The selection of each objective functions and constraint was discussed in sections 2.2 and 2.3, and the overall problem formulation was presented in section 2.4. Variability and uncertainty compensation can be further improved by selecting an advanced control technique that relies on short-term load and wind forecasting and by suitable time step and horizon selection for the OC strategy. This will be discussed in detail in the following section.

3. MODEL PREDICTIVE CONTROL BASED ALGORITHM

3.1 Introduction

The impact of variability in wind and load on operations are more pronounced in isolated power systems with low inertia and high penetration of wind generation. As discussed in section 1, most of the existing solution techniques do not consider look-ahead capability to foresee how present decisions can influence response capability of the dispatchable DERs at a future time. In addition, the approaches do not incorporate feedback capability to compensate for increased uncertainty in isolated power systems with relatively large amounts of renewable generation. The focus of this section is to present the OC problem formulation proposed in section 2 in the framework of the chosen solution technique, which addresses the drawbacks of existing methods.

Adaptive dynamic programming (ADP) and model predictive control (MPC) are possible solutions techniques for the OC problem. The advantages and disadvantages of two techniques are discussed in section 3.2.1, in terms of computational complexity, the objective function value and in compensating uncertainty in the problem. Both approaches can perform online optimization and have a way of accounting for variability and uncertainty. In this work, MPC was chosen over ADP because finding suitable value function approximations for the ADP is a cumbersome task and computational complexity is not a concern for the OC problem being addressed, as long as the mathematical program is convex.

MPC is able to handle issues associated with high penetration of renewables in low inertia systems, variability due to wind/load, and uncertainty due to forecasts in wind, load and large disturbances as discussed in section 3.2.2 and 3.2.3. This is because at every step a finite horizon optimal control problem is solved using feedback from the system. In section 3.3, a mathematical formulation of the OC problem in the MPC framework is given. More specifically, the predictive model, cost function and constraints which are the key elements of the MPC optimizer are defined for the OC problem. The co-simulation was setup for evaluating the approach and for investigating time scale coupling of the OC strategy with lower level frequency controls is described in section 3.4. A summary of this section is presented in section 3.5.

3.2 Solution technique selection for optimal dispatch and coordination problem

Adaptive dynamic programming and model predictive control are two modern approaches used to solve dynamic optimization problems. Both MPC and ADP have the ability to perform online optimization and have a way of avoiding the "curses of dimensionality" associated with dynamic programming approaches. MPC has already had a huge impact on control practices, especially in the process control area [57, 58] and has also been applied to an economic dispatch problem [19]. The theory on ADP is not as developed as MPC, but is showing much promise for many applications, including power systems, communication systems, generators, missile systems, logistics, operations research [58-61]. ADP has been demonstrated to be a good solution method for a small class of problems, such as complex resource allocation problems (i.e., transportation problems), playing games (i.e., backgammon), and solving engine control

problems (i.e., managing fuel ratio mixtures in engines) [60]. Online optimization is important for an isolated microgrid because of the increased uncertainty and variability caused by high penetration of wind generation, along with the fact that relatively low inertia systems are vulnerable to disturbances. Both the MPC and ADP methods are discussed next, followed by a comparison between the two approaches.

3.2.1 Comparison of MPC and ADP solution techniques

In this section, a justification is given for the preference of using MPC over ADP as a solution technique for the OC problem. The advantages and disadvantages of two techniques are discussed in terms of computational complexity, ease of defining the objective function value and ability to compensate for uncertainty in the system. Even though both MPC and ADP have the ability to perform online optimization and have a way of bypassing the curses of dimensionality associated with DP, the MPC approach could become computationally expensive if solving large-scale mathematical programs especially if the problem is non-convex. For the OC problem formulated in this work, the mathematical program is not considered to be large scale, especially for relatively small isolated systems with less than 10 DERs committed. Therefore, computational complexity would not be an issue if using MPC. Depending on the method chosen to approximate the expectation of the value function, ADP replaces the computational burden of looping over all possible states with a statistical problem caused by estimating the value of visiting each probable state [60]. However, for a small class of problems, the estimation of the value function can be simple where substantial computational complexity can be avoided [60]. It is unclear whether the OC problem fits within the

small class of problems, so estimation of the value function could potentially be an issue of the ADP approach is used.

For the most part, MPC is formulated and analyzed as a deterministic problem that utilizes short term forecasts [19], although it can still be effective for stochastic problems because it is able to react to new uncertainty using feedback. ADP may seem to have an advantage over MPC because it proactively accounts for uncertainty using statistical information, however, finding value approximations that are suitable for a specific problem can be an unwieldy task [60].

3.2.2 Benefits of using MPC for solving the OC problem

For the optimal coordination problem at hand, either MPC or ADP could be used to address the issues of increased variability and uncertainty associated with high renewable penetration. This is because both can perform online optimization and have a way of systematically accounting for variability and uncertainty. In this work, MPC was chosen over ADP because computational complexity is not a concern for the OC problem being addressed, as long as the mathematical program is convex. However, finding suitable value function approximations for the ADP is a cumbersome task. In the MPC approach, at every step a finite horizon optimal control problem is solved using feedback from the system [19, 57]. The control action at each step is computed on-line instead of using a pre-computed, off-line, control law. In this manner, MPC is considered closed loop and has the ability to compensate for additional uncertainty and variability caused by high penetration of renewable energy resources.

3.2.3 Description of model predictive control

Model predictive control (MPC) is an online receding horizon optimization control technique. This method was introduced in the 1970's to effectively and systematically solve constrained multivariable control problems, which are common in process control industries [58]. Fig. 7 shows the different components of the MPC control method.

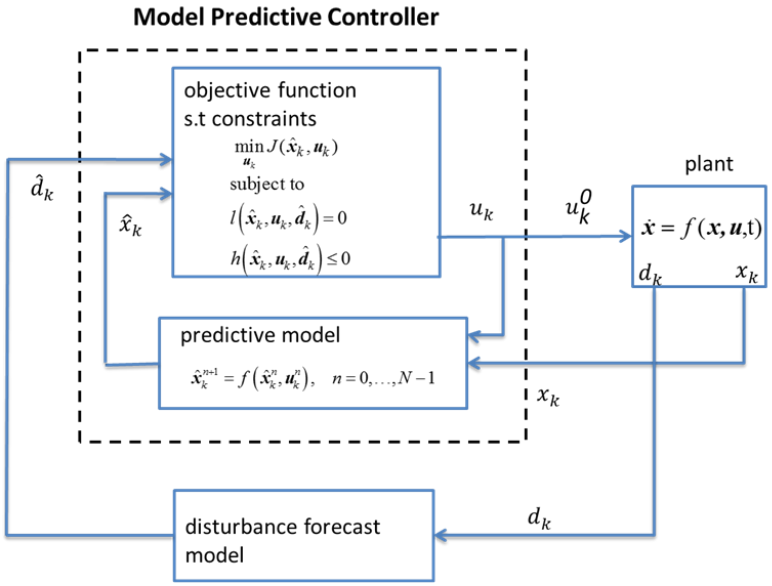

Fig. 7 Structure of Model Predictive Control

The model predictive controller solves, at every time step, a finite horizon optimal control problem using feedback from the system [19, 57]. However, the control sequence is implemented for only one step ahead. The model predictive controller contains all the elements of an optimal control problem, which is categorized under the

umbrella of a dynamic optimization. As shown in Fig. 7, the main components of MPC are: the objective function, constraints, and predictive model of the system. $\boldsymbol{x}_k, \boldsymbol{u}_k^0, \boldsymbol{d}_k$ are the state, control, and disturbance variables associated with a plant or system at decision step k with $k = 0,\ldots,K-1$, where K is the optimization horizon. A forecast model is typically used to predict the disturbances $\hat{\boldsymbol{d}}_k = \left[\hat{\boldsymbol{d}}_k^0 \;\; \hat{\boldsymbol{d}}_k^1 \cdots \hat{\boldsymbol{d}}_k^{N\text{-}1}\right]$ over the prediction horizon N. $\hat{\boldsymbol{d}}_k$ is then used as an input to the model predictive controller. The control objective of the model predictive controller is to find a sequence of predicted control inputs $\boldsymbol{u}_k = \left[\boldsymbol{u}_k^0 \;\; \boldsymbol{u}_k^1 \cdots \boldsymbol{u}_k^{N\text{-}1}\right]$ over a given prediction horizon such that the objective function in (14) is minimized and the constraints represented by (16) are satisfied. After the initial conditions $\hat{\boldsymbol{x}}_k^0 = \boldsymbol{x}_k$ are specified, the sequence of predicted states $\hat{\boldsymbol{x}}_k = \left[\hat{\boldsymbol{x}}_k^1 \;\; \hat{\boldsymbol{x}}_k^2 \cdots \hat{\boldsymbol{x}}_k^N\right]$ at each step over the prediction horizon is determined using the predictive model defined in (15). The first control input $\boldsymbol{u}_k^0$ of the control sequence $\boldsymbol{u}_k$ is applied to the plant/system, and the states are measured at the next decision step to obtain $\boldsymbol{x}_{k+1}$. The process is repeated with measurement of $\boldsymbol{x}_{k+1}$ serving as an initial condition to compute the control at the next step $\boldsymbol{u}_{k+1}$. The model predictive controller can be described mathematically by (14), (15), and (16).

$$\min_{\hat{\boldsymbol{u}}_k} J = \sum_{n=1}^{N-1} J_n(\hat{\boldsymbol{x}}_k^n, \boldsymbol{u}_k^n) + J_N(\hat{\boldsymbol{x}}_k^N) \tag{14}$$

subject to:

$$\hat{\boldsymbol{x}}_k^{n+1} = f\left(\hat{\boldsymbol{x}}_k^n, \boldsymbol{u}_k^n, \hat{\boldsymbol{d}}_k^n\right), \qquad n = 0,\ldots,N-1 \tag{15}$$

$$l\left(\hat{\boldsymbol{x}}_k^n, \boldsymbol{u}_k^n, \hat{\boldsymbol{d}}_k^n\right) = 0, \qquad n = 1, \ldots, N$$
$$h\left(\hat{\boldsymbol{x}}_k^n, \boldsymbol{u}_k^n, \hat{\boldsymbol{d}}_k^n\right) \le 0, \qquad n = 1, \ldots, N \tag{16}$$

$f(\cdot)$ and $g(\cdot)$ are the functions relating state, control and noise variables to the states in the next step and outputs respectively. $l(\cdot)$ and $h(\cdot)$ are the equality and inequality constraints on the state, control and noise variables. The dynamics of the predictive model and constraints given in (15) and (16) are then computed at every decision step $k = 0,1,\ldots,K-1$.

3.3 Optimal coordination using the MPC framework

In this section, the overall mathematical formulation of the optimal coordination problem formulation, presented in section 2.4, is re-written in the MPC framework. Also, a simple example is presented illustrating how MPC can be used to solve the OC problem. The interaction between MPC and an isolated microgrid is shown in Fig. 8. More specifically the predictive model, objective function and constraints, as shown in Fig. 8, constitute the elements of the model predictive controller were defined in terms of the OC problem formulation discussed in section 2.4. The isolated microgrid (or plant) represents a dynamic system containing the primary controls, operating at continuous time t and time frame T_p. The model predictive controller represents the tertiary controls operating at discrete time step k.

The state variable vector $\boldsymbol{x_k}$ represents the measurement outputs from the isolated microgrid system at decision step k. It consists of state-of-charge of the battery

storage. The control variable vector $\boldsymbol{u}_k^0$ represents the power setpoints of the diesel generators, power setpoints of battery energy storage, storage reserve power and wind power curtailed, implemented at decision step k. The wind and load power are represented by the disturbance term $\boldsymbol{d}_k$. The disturbances are predicted using a forecasting method.

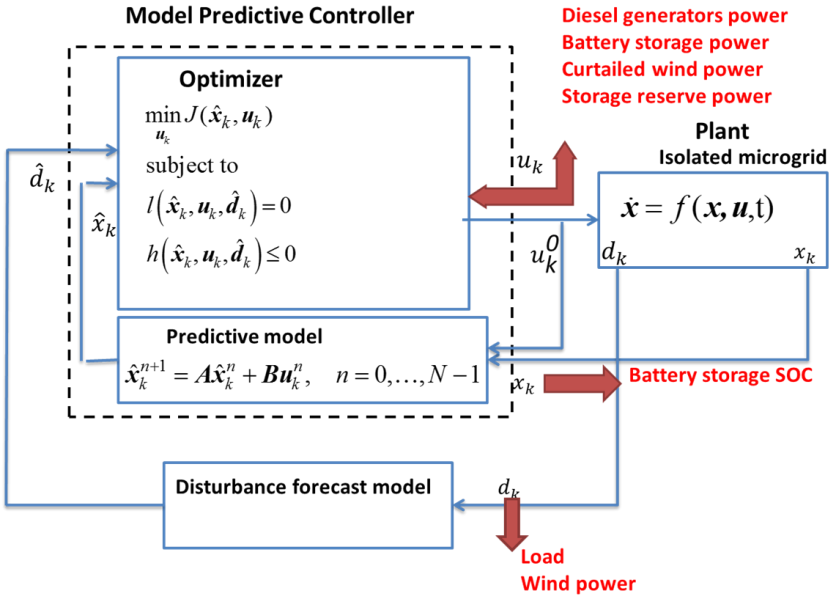

Fig. 8 Interaction between model predictive controller and isolated microgrid

The overall mathematical formulation can be written in the MPC framework, in terms of the different components such as the optimizer (cost function and constraints) and predictive model components.

Predictive Model: A predictive model representing the state trajectories was expressed by the difference and algebraic equations given in (17).

$$SOC_i\left(k+n+1|k\right) = SOC_i\left(k+n|k\right) - \alpha_i \hat{P}_{si}\left(k+n|k\right),\ i=1,\ldots S \tag{17}$$

SOC_i is the predicted state-of-charge of the *i*-th energy storage.

Constraints: The constraints, discussed in section 2.3, on reserve requirements for the energy storage, the power output levels of the energy storage and diesel generators, and the curtailed wind power, and power balance are given in (18).

$$\begin{aligned}
&\sum_{i=1}^{S}\hat{P}_{si}\left(k+n|k\right)+\sum_{j=1}^{G}\hat{P}_{Gj}\left(k+n|k\right)-\hat{P}_{curtail}\left(k+n|k\right)=\hat{P}_L\left(k+n|k\right)-\hat{P}_W\left(k+n|k\right)\\
&-\sum_{i=1}^{S}\hat{P}_{URSi}\left(k+n|k\right)\le-\Delta P\left(k\right)\\
&\hat{P}_{si}\left(k+n|k\right)+\hat{P}_{URSi}\left(k+n|k\right)\le-P_{si}^{\max}\\
&-\hat{P}_{si}\left(k+n|k\right)\le-P_{si}^{\min}\\
&-SOC_i\left(k+n+1|k\right)\le-SOC_i^{\min}\\
&SOC_i\left(k+n+1|k\right)\le 1\\
&\hat{P}_{Gj}\left(k+n|k\right)\le P_{Gj}^{\max}\\
&-\hat{P}_{Gj}\left(k+n|k\right)\le-P_{Gj}^{\min}\\
&\hat{P}_{curtail}\left(k+n|k\right)\le P_{curtail}^{\max}\\
&-\hat{P}_{curtail}\left(k+n|k\right)\le 0\\
&-R_{Gj}^{\max}\le\Delta P_{Gj}(k)\le R_{Gj}^{\max}
\end{aligned} \tag{18}$$

$\hat{P}_{Gj}$ is the predicted power output of the *j*-th diesel generator, $\hat{P}_{si}$ is the predicted power level of the *i*-th energy storage unit, $\hat{P}_{URSi}$ is the predicted up reserve requirement on the *i*-th energy storage unit and $\hat{P}_{curtail}$ is the predicted amount of curtailed wind power. $\hat{P}_L$

and $\hat{P}_w$ are the forecasted wind and load in the system, $\Delta P(k)$ is the power output of the largest diesel generator at decision step k. $P_{si}^{\min}$ and $P_{si}^{\max}$ are the lower and upper limits on the *i*-th energy storage unit's predicted power output. $SOC_i^{\min}$ is minimum state-of-charge of the *i*-th energy storage unit. $P_{Gj}^{\min}$ and $P_{Gj}^{\max}$ are the lower and upper limits on the *j*-th diesel generator's predicted power output. $R_{Gj}^{\max}$ is the maximum allowed power change of the j-th diesel generator from one time step to the next. $\hat{P}_L$ and $\hat{P}_w$ are the forecasted load and wind in the system.

Objective function: The objective function at the *n*-th prediction time step is defined based on a weighted combination of the fuel cost and the wind curtailed objective and is defined in (19).

$$\min \hat{J}_k = \sum_{n=1}^{N-1}\left[\sum_{j=1}^{G}\left(a_j + b_j\hat{P}_{Gj}\left(k+n|k\right) + c_j\hat{P}_{Gj}^2\left(k+n|k\right)\right) + d\hat{P}_{curtail}\left(k+n|k\right)\right]\Delta t \tag{19}$$

3.4 Approach for evaluating multi-time scale coordination strategy

Since time scale separation is typically assumed between economic dispatch and lower level frequency controls (e.g., primary frequency controls), static approaches have been commonly used to evaluate tertiary control approaches. To ensure coordination between the different layers of control in the presence of high variability and uncertainty, it is necessary to capture electromechanical behavior of the power system under study in response to setpoint changes from a tertiary controller.

There are many commercially available simulation software tools with the appropriate capabilities for studying the electromechanical behavior for transmission and distribution level power systems. These tools include DiGSILENT PowerFactory [62], PSCAD/EMTDC® [63]Power System Toolbox (PST)[64], and PSS®E [65]. Some of these tools even contain traditional economic dispatch and optimal power flow solvers that can be applied to static or quasi-steady state problems. However, it is not straightforward to modify these power system simulation packages to implement newly developed tertiary control strategies and to study the interaction of the tertiary controls with primary control dynamics which occur at shorter time scales. For this reason, a co-simulation was setup using DiGSILENT PowerFactory and MATLAB to allow power setpoint changes $\boldsymbol{u}_k^0$, output measurements $\boldsymbol{x}_k$ and disturbance measurements $\boldsymbol{d}_k$ to be exchanged between the model predictive controller designed and the isolated power system dynamics, as shown in Fig. 8. DiGSILENT PowerFactory was used to simulate dynamical behavior the isolated power system under study. For dynamical simulations, a time step of 0.001s was selected. The MATLAB optimization toolbox was used for modeling the behavior of the model predictive controller. To run co-simulations an automated batch process was created for data exchanges between the DiGSILENT and MATLAB. MATLAB was used as the master for initiating and terminating the co-simulations, as well as, initiating the batch process at every decision step k. This co-simulation setup enabled the impact of the OC strategy on economic operation and technical performance, such as, frequency performance to be investigated.

3.5 Summary

In section 3.2, model predictive control and adaptive dynamic programming were reviewed and compared as two possible modern optimal control techniques that can be used to solve the optimal coordination problem. Given the complexity of finding suitable value function approximations needed for the ADP approach, MPC was chosen to solve the optimal coordination problem formulated. Section 3.3 presents the OC problem formulation defined in section 2.4 in the MPC framework. The method used to evaluate the effectiveness of the OC strategy and investigate time scale coupling with lower level controls is described in section 3.4. In the next section, simulation studies are presented after applying the MPC based OC method to an isolated microgrid test system. Recommendations are also given to for extending the proposed OC strategy and designing multi-time scale optimal coordination strategies to other classes of isolated power systems with significant levels of variability and uncertainty in loads and/or renewable generation.

4. NUMERICAL SIMULATION AND DISCUSSIONS

4.1 Introduction

The proposed formulation and the solution algorithm for optimally coordinating DERs in an isolated system with high penetration of renewable energy resources was presented in sections 2 and 3. The objectives were to simultaneously minimize operating costs of diesel generators and maximize the utilization of wind generation, while considering equipment life of DERs, physical limitations on the individual controllable resources and maintain adequate frequency performance. Model predictive control was proposed as a solution method to solve the optimal coordination strategy since it has the features of periodic feedback and look-ahead capability allowing for compensation of increased variability and uncertainty linked to high penetration of renewables.

The focus of this section is to study the effectiveness of the MPC based optimal coordination strategy by performing extensive simulation studies on a transient isolated microgrid model under realistic scenarios. Performance metrics are defined in section 4.2 in terms of economics, technical performance and computational time. A description of the isolated microgrid test system including the models of the different DERs is given in section 4.3. The test cases, used to study the effectiveness of the MPC based OC strategy, are described in section 4.4. Finally, the performance of the MPC based OC strategy is studied in section 4.5 in by varying the time step and the prediction horizon. Several studies were performed to demonstrate the impact of these parameters in terms of the performance metrics.

4.2 Performance metrics

Metrics were selected to evaluate the performance of the OC strategy in terms of economic performance, technical (system frequency) performance, and computational time. Due to under- and over- forecasting, the "actual" cost from the system could be lower or higher than the predicted cost determined by the model predictive controller. Therefore, instead of using absolute cost to evaluate economic performance, the average error between actual and predicted costs J_{MAE} as given in is used to assess whether the coordinated DERs are operating close to optimal or economic setpoint, which is represented by,

$$J_{MAE} = \frac{1}{K}\sum_{k=1}^{K}\left|\hat{J}_k(\hat{x}_k^1) - J_k(\bar{x}_k)\right| \tag{20}$$

where $\hat{J}_k$ and J_k are the predicted cost based on the model predictive controller outputs and actual cost based on system response at time step k, respectively, $\hat{x}_k^1$ is the first element of the sequence of predicted states over the prediction horizon, $\bar{x}_k$ is average state measurements from system over time step k, and K is total number of time steps over the length of time considered.

The North American Electric Reliability Corporation (NERC) BAL-001-2 is a standard that was developed for managing frequency control performance in the short-term to maintain reliability in an interconnected power system. This standard currently uses area control error (ACE) and Balancing Authority ACE Limits (BAAL) to measure frequency control performance of individual control area relative to the larger system

[66]. For this work, the BAAL was adapted for a single area system to evaluate technical performance in terms of frequency control performance and is given as follows:

$$(FTL_{low} - 60) \leq \Delta f_{1\min} \leq (FTL_{high} - 60) \tag{21}$$

where FTL_{low} and FTL_{high} are the specified low and high frequency trigger limits. $\Delta f_{1\min}$ is the 1-min average frequency deviation sampled every second. In particular, the metric used to evaluate frequency control performance is total time of violations in 1-min average frequency deviations in (21), as a percentage of the total time period of interest (e.g., 4hr). FTL_{low} and FTL_{high} have been defined for each major interconnection in North American interconnected power system, but not for small scale isolated power systems. However, the Electric Reliability Council of Texas (ERCOT) system is classified as an isolated power system because of its weak ties with the larger interconnected system. Since the ERCOT system is closest to the class of systems focused on in this work, FTL_{low} and FTL_{high} were selected to be 59.91 and 60.09 Hz, respectively, based on limits specified for the ERCOT system. Because this is considered to be a large scale isolated power system, these limits can be seen as conservative limits for small scale isolated power systems.

The average computational time taken by the model predictive controller to compute new setpoints at each time step was used to assess computational impacts of varying important parameters such as time step and prediction horizon. Changes in these parameters will impact the number of decision variables and constraints, which in turn, affects computational burden.

4.3 Test system description and parameters

To study the impact of the OC strategy on the system frequency performance, defined in section 4.2, it was pertinent to ensure that the test system model captures system frequency behavior in response to changes in wind, load and dispatch setpoints. Therefore, a dynamic model of an isolated microgrid test system was developed using DIgSILENT PowerFactory [62] for the studies. A schematic of the model, which is based on a modified version of the IEEE 123-node distribution radial test feeder [67] is shown in Fig. 9. In order to represent a microgrid in isolated mode, the test feeder was disconnected from all substations at nodes 150, 251, 195 and 451, and DERs were placed within the system at specific nodes. The legend summarizes the DER locations, types, and ratings. Also, a controllable dump load was placed at node 60 in the proximity of the wind generators to execute the wind curtailment function.

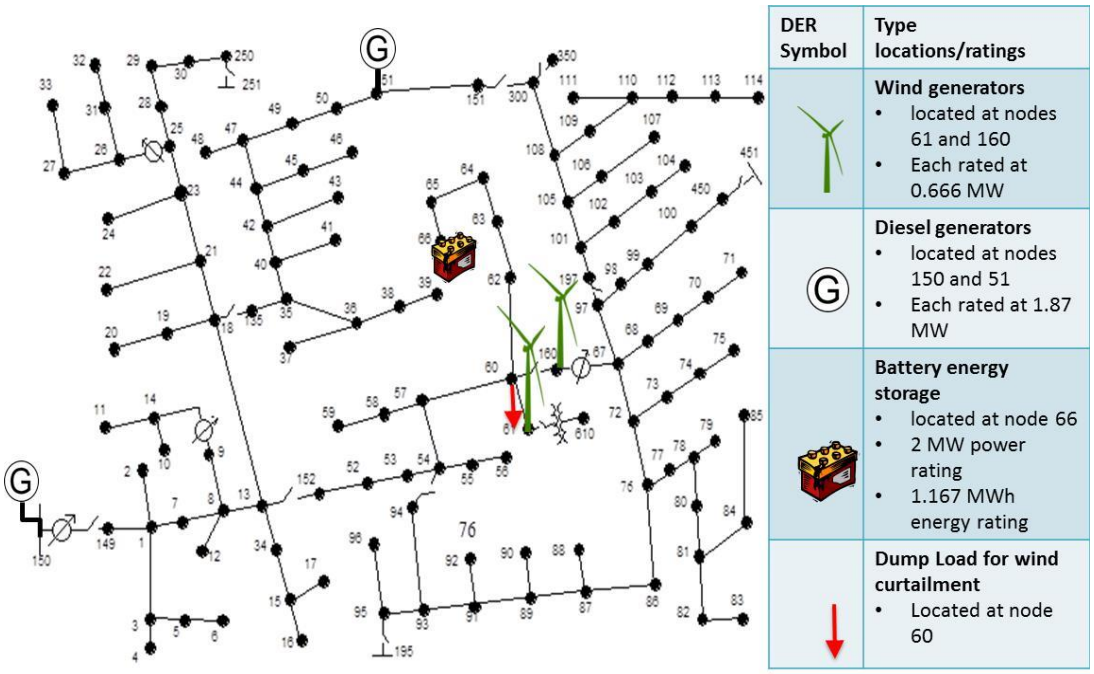

Fig. 9 Isolated microgrid test system (modified and reprinted with permission from [67] © 2010 IEEE)

Standard models for diesel generators, battery energy storage, wind generators, controllers, and dump load were chosen for the DERs. These models and the parameters selected for the studies will be discussed in the following subsections.

4.3.1 Diesel generator system model

The diesel generator was represented by a combination of a synchronous generator, diesel governor and exciter. The synchronous generator is used to convert the mechanical power output from a diesel engine to electrical power. Synchronous generator models are well studied in the literature. A standard model was used in this work, as given in [68]. Synchronous machine parameters were selected according to the

Marelli Generators specifications for the 2.34 MVA rated 3-phase generator model (MJB 500 LA 6) with inertia of 88.9 kgm^2, as given in [69].

The mechanical power output of diesel engine is typically controlled by a speed governor in response to speed deviations from a reference speed. The speed governors are typically equipped with primary frequency droop control to allow stable load sharing amongst two or more synchronous machines operating in parallel. One common diesel governor is the Woodward governor that consists of a speed sensor, hydro-mechanical actuator and a diesel engine. This common model is used in this work and is also commonly known as DEGOV1. More details regarding the model are provided in [70]. The output signal of the speed sensor is first conditioned and amplified. The actuator then adjusts the valve position of the fuel supply to regulate the engine power output until the system frequency is stabilized.

The terminal voltage of a synchronous generator can be controlled by an exciter system. A simplified excitation system (SEXS) was modeled in this work, as given in [70]. This model represents the general characteristics of a wide range of properly tuned excitation systems and is useful when its detailed design is unknown. Parameters for the DEGOV1 and SEXS were selected based on guidelines given in [71].

4.3.2 Battery energy storage system model

A battery energy storing system (BESS) consists of two parts [72]: 1) a battery representing the electrochemical process to store and release energy and 2) a rectifier/inverter that converts the DC-voltage from the battery to the AC-voltage needed for the grid and vice versa. The BESS modeled, shown in Fig. 10 was taken from the

DiGSILENT PowerFactory library and consists of the battery connected to the rectifier/inverter through a DC voltage bus [72]. The rectifier/inverter is an IGBT-based converter, in which d-q axis current parameters are controlled corresponding to the active and reactive power of the BESS.

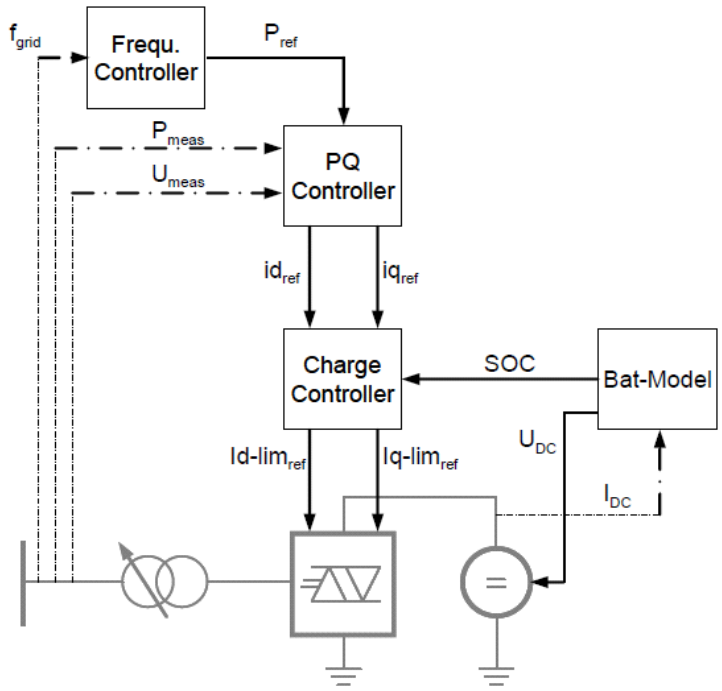

Fig. 10 Battery energy storage system (reprinted with permission from [72])

The charge controller limits the power injections from the BESS to the network given the power references determined by the PQ controller and the SOC of the battery model. The PQ controller is modeled by a PI controller and decides the appropriate d-q current references based on measured power and voltage from the AC bus that the BESS

is connected to, as well as, the power reference determined by the frequency controller. The original model was designed to investigate BESS behavior when providing primary control support. Modifications to the original model were made so that the active power reference of the BESS can be changed according to an external signal from a tertiary controller in addition to the reference determined based on frequency droop characteristics of the primary controller. Default settings were used for the BESS controllers. Parameters for the battery model were chosen from [73].

4.3.3 Wind generator model

Because doubly fed induction generator (DFIG) variable speed generators have become the popular type amongst the installed wind turbines, this type of wind generator was modeled. Typically, variable speed wind generators are able to achieve maximum aerodynamic efficiency by adjusting the rotational speed of the wind turbine based on constantly changing wind speeds [9]. A DFIG type wind generator consists of a wound rotor induction generators (WRIG) with the stator directly connected to the electrical grid and the rotor controlled by a bi-directional partial scale power converter [74]. The partial scale power converter is commonly 30% of the nominal generator power and also limits the range of variable speed control to be ±30% of the synchronous speed. DFIG behavior is governed by the power converter and controllers in normal and fault conditions. The power converter controls the rotor voltage magnitude and phase angle for active and reactive power control [74]. The DFIG model used in this work was obtained from the DIgSILENT Powerfactory library, and is explained in more detailed in

[75]. Default control parameters were used, but ratings and wind speed characteristic curves were specified based on [76].

Test cases were developed to evaluate the proposed MPC based OC strategy under realistic scenarios. Wind speed data was obtained from the Columbia Basin Wind Energy Study (CBWES) for the period July 28 - August 11, 2011. Wind speeds were captured from a sonic anemometer at two levels (60 m and 30 m) above ground located in northeastern Oregon. The CBWES data is not publically available. This wind speed data is then used as input to the wind generators modeled in DIgSILENT PowerFactory software to modulate the wind power output.

4.3.4 Load models

Time series data was also needed for the spot loads during the simulations to represent load variations. The time series load data was obtained from a simulation of a population of residential loads in GridLAB-D an open-source distribution system software [77]. Residential loads were modeled using a combination of detailed physical models of air-conditioners and water heaters as well as static, voltage dependent time-series load models to represent all other appliances. In the physical models, an equivalent thermal parameter (ETP) model was used, which has been demonstrated to be an accurate representation for residential home instantaneous power demand and energy consumption. For more details on the ETP model, refer to [78]. The behavior of the residential population is typically driven by weather. Therefore, it was assumed that the residential population was also located in northeastern Oregon to make sure the load and wind data reflect netload (total load minus total wind generated) disturbances in a

particular area. Using the load data for the IEEE 123-node system, the residential load models were populated and parameterized using the method described in [79]. Specifically, the time series data for the aggregate load at each node was obtained and used as inputs to vary the load in the study cases.

When excess wind generation is produced, additional generation can be directed to dump loads. Common examples of dump loads are resistive loads such as standby resistive loads, community heating, hot water heaters, etc. In this work, a dump load is modeled as a static constant power load, where the power consumption is varied by an external or tertiary control signal. It is assumed that the dump load is controllable and dispatchable.

4.4 Test cases description

After obtaining the wind and load datasets (as discussed in section 4.3.3 and 4.3.4), it was discovered that persistent up and down ramps in net load power output occurred within a 2-3 hr. period. Based on this observation, several 4 hr. profiles with interesting trends in netload variations were studied. The two netload datasets considered are shown in Fig. 11. Dataset A has an hourly netload trend, increasing ~1600 kW over a 2hr period and ±600 kW variations within a 1min time frame. In dataset B, the netload varies as much as 1500 kW over a 1 min time frame and has a fairly constant hourly trend. The average wind penetration level for both datasets was 45%. These variations and penetration levels could cause significant error in netload forecast even in the short term, as well as, have an impact on system economics and technical performance, especially if DERs are not coordinated appropriately.

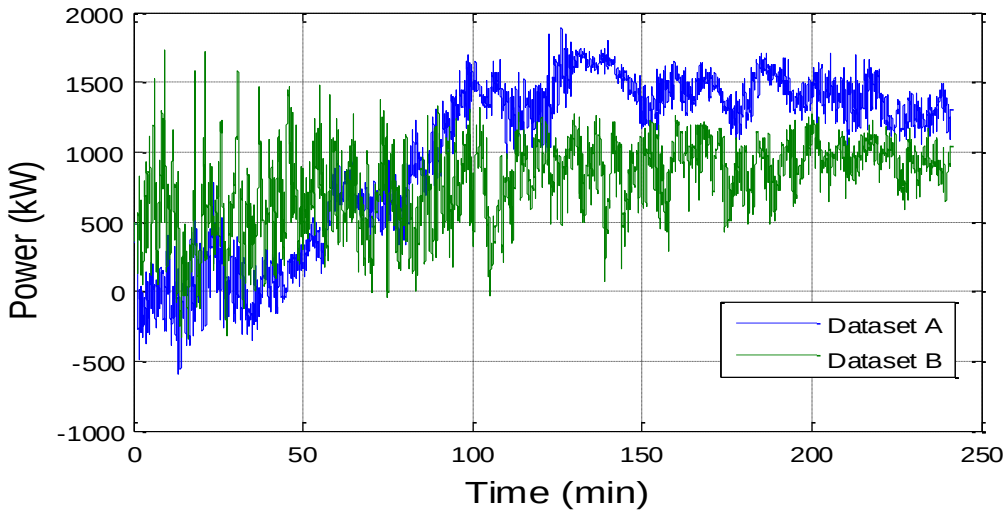

Fig. 11 Netload for datasets A and B

In the model predictive controller, upper limits on power output and SOC were selected based on the physical limits of the diesel generators and battery energy storage included in the microgrid test system. However, the lower limit on each diesel generator's power output was selected to be ~561 kW, which was 30% of the rated power, to avoid generator cycling and inefficient operation of the diesel generators. The minimum SOC for the battery energy storage was selected to be 0.4 to avoid impact on battery life degradation. Ramp rate limits on diesel generator power output were not considered.

4.5 Results and discussions

In the studies, the time step and prediction horizon of the OC strategy were varied for each dataset selected in section 4.4. The studies investigated the effectiveness

of the OC strategy in compensating for the variability and uncertainty due to high penetration of wind generation in isolated systems using the performance metrics defined in the previous section. Also, due to selecting smaller time steps for the OC strategy, the coupling with the primary frequency control time scale was investigated.

4.5.1 Varying time step

The time step was varied from 10 s to 10 min and the prediction horizon was kept constant at 10 min. For dataset A, Table 1 summarizes the economic performance (J_{MAE}), technical performance (average frequency violations), and average computational time, which were the performance metrics defined in section 4.2. The results for each category of performance will be discussed in detail next.

Table 1 Summary of technical performance, economics and computational time for dataset A with varying time step

Time step	J_{MAE} *($)*	*Average Freq. Violations (%)*	*Average Computational time per step (s)*
10 s	1.998	0.81	0.161
15 s	2.352	1.51	0.054
20 s	2.667	6.27	0.035
30 s	2.71	8.49	0.025
60 s	3.572	18.15	0.014
5 min	6.8622	37.73	0.010
10 min	13.1923	52.31	0.016

As indicated in Table 1, J_{MAE} decreases as the time step is reduced. A persistent predictor was used to forecast the netload in which the forecasts for all future time steps were set to the current value of the variable being predicted. It essentially replicates the actual data, with a lag of one period. The advantage of the naïve approach is that it is simple to implement. Its major weakness is its inability to make highly accurate forecasts if there are significant changes from one period to the next. As a result, the forecast error became larger as the time step increases due to larger variations in netload between time steps. This can be seen from Fig. 12 in which the actual and forecasted netload (obtained using the naïve predictor) for the 10 s time step case is compared to the 10 min case. Quantitatively, the Mean Absolute Error (MAE) between actual and forecasted netload at each time step was used to capture changes in uncertainty. For dataset A, the MAE of the netload forecasted increased from 65 kW to 161 kW as the time step increased from 10s to 10min. Hence, for shorter time steps, the actual responses of the DERs in the system are closer to the optimal setpoints determined by the model predictive controller leading to a smaller J_{MAE}.

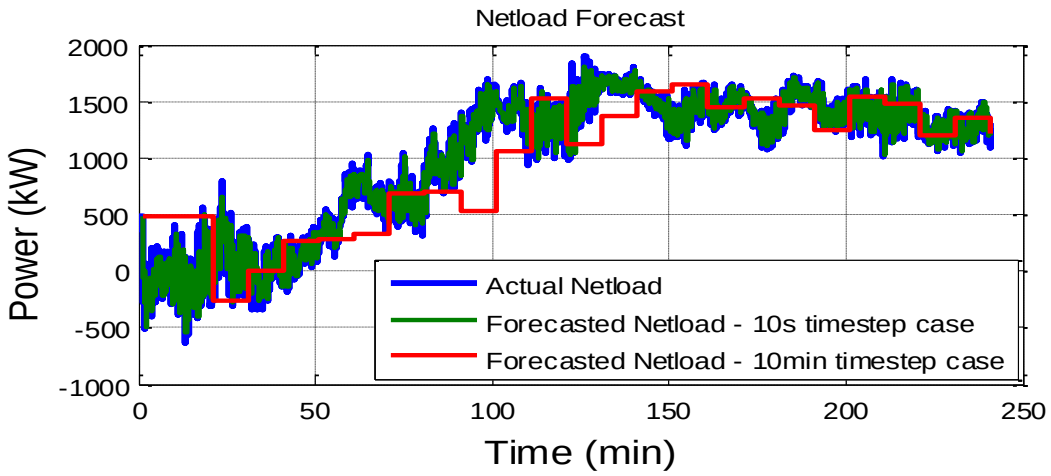

Fig. 12 Actual vs. forecasted netload for 10 s time step and 10 min time step cases

Table 1 also shows the average frequency violations increase as the time step gets larger. This can be further demonstrated in Fig. 13 which shows a comparison of 1-min average frequency deviations over time between the 10 s and 10 min time step cases. The average frequency was kept within the specified bounds 99% of the time in the 10s case while the average frequency was held within bounds only 48% of the time in the 10min case. In summary, the average frequency performance is improved significantly by dispatching faster since power can be better balanced and net load variations can be matched in the presence of considerable variability.

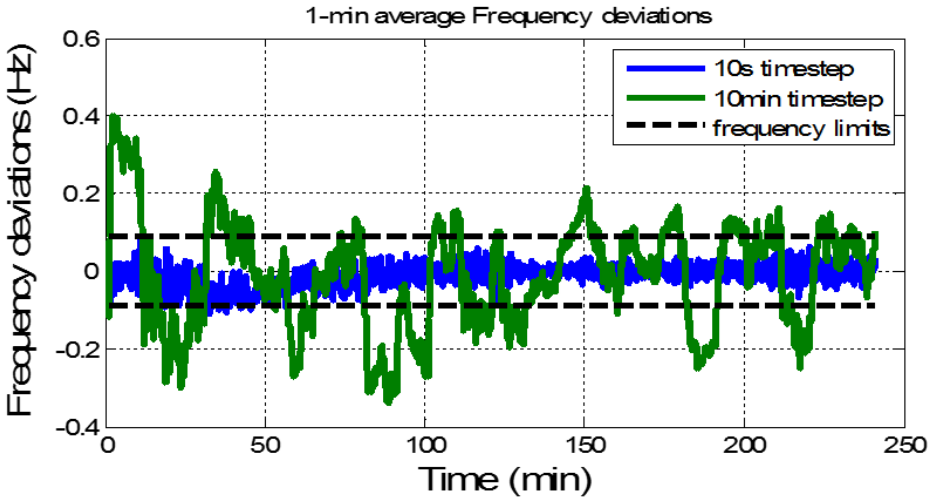

Fig. 13 1-min average frequency deviations sampled every second for 10 s and 10 min cases for dataset A

On the other hand, the computational time increased with the length of the time step, as seen in Table 1, because a smaller time step leads to increased decision variables and constraints over the same prediction horizon (i.e., 10 min). For a 10 min prediction horizon, with a 10 s time step, the number of decision variables and constraints were 660 and 600, respectively. In the 30 s time step case with the same 10 min prediction horizon, the number of decision variables and constraints were 1/3 of the total number of variable of the 10 s case. The computational time to calculate setpoints increased to ~0.16 s per step using a 10 s time step from ~0.02 s per step using a 30 s time step. However, 0.16 s per step is still reasonable since the time step was 10 s and major changes in netload do not occur within this time period.

As is shown from Table 2, for dataset B, the same trend was observed as in dataset A in terms of increased average frequency violations and J_{MAE} as the time step

was increased. Conversely, results were not obtained for the 5 min and 10 min time step cases. This is because the dynamic simulations failed to converge after some time, due to a combination of the large netload variations and battery storage local control settings. For instance, the PQ controller of the storage used PI controllers whose performance is sensitive to the gain parameters selected. Also, the charge controller settings limited the switching between charge and discharge within a 30 s timeframe. The settings of the charge controller and P-Q controller were not tuned appropriately for all operating conditions, since designing primary controllers for DERs was not the focus of this work. As a result, the battery storage controls tend to over-compensate for large disturbances thereby saturating and causing integral windup which leads to non-convergence in solutions leading to the simulations failing.

Table 2 Summary of technical performance, economics and computational time for dataset B with varying time step

Time step	J_{MAE} *($)*	*Average Freq. Violations (%)*	*Average Computational time per step (s)*
10 s	2.682	1.03	0.1507
15 s	3.284	4.27	0.0666
20 s	3.723	11.55	0.0404
30 s	4.154	19.65	0.0235
60 s	5.679	38.84	0.0105
5 min	N/A	N/A	N/A
10 min	N/A	N/A	N/A

According to the results, the 10 second time step leads to the best economic and average frequency performances, as well as, a reasonable computational time given the input variability from the wind and load. However, there are some concerns that this time step is within the primary control timeframe, so further investigation into coupling between time scale implementation of the OC strategy and primary frequency controls is needed to understand the impact on primary control performance. Time scale coupling impacts are discussed in the next subsection.

4.5.2 Coupling between fast dispatch and primary frequency controls

Before proceeding to study the coupling between the OC strategy and the primary controls, the time frame of the primary controls should be determined. The time frame of primary controls for the microgrid test system defined in section 4.3 was determined through studies. For each study, a transient simulation, where the diesel generator located at node 51 operating at 0.5 MW is tripped at 20s. In the base case, the frequency droop settings of the diesel generator governors were 0.05 p.u. The battery energy storage model also includes a frequency droop controller with a droop setting of 0.05 p.u and frequency deadband of 0.0012 Hz. The deadband helps to avoid constant charge and discharge due to continuous frequency fluctuations. The system frequency response is shown in Fig. 14.

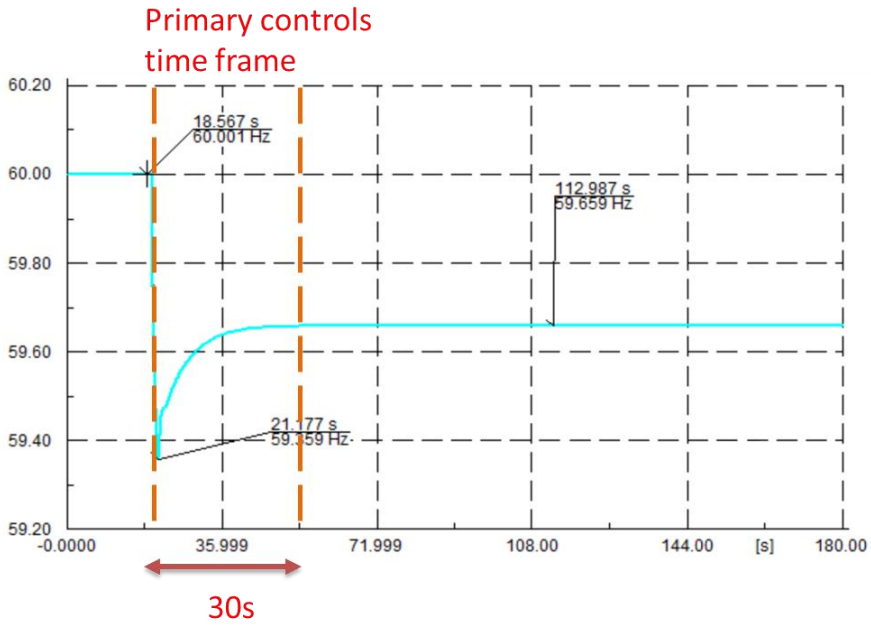

Fig. 14 System frequency response to diesel generator outage at node 51

After the diesel generator is tripped the fast acting battery storage unit ramps up to compensate for the generation lost, which helps to arrest the system frequency at 59.36 Hz. The diesel generator outputs are then adjusted to aid in stabilizing system frequency. After approximately 30s, the system frequency reaches a new steady state. Since the diesel generators have a much slower response (e.g., seconds) than battery energy storage (e.g., milliseconds), the time to reach a new steady state following a disturbance is dominated by the response of diesel generators. This can be further seen simply by changing parameters of the storage frequency controllers that affect the response time of the BESS, such as, droop or deadband settings. In the following set of studies, it is shown that modifying storage deadband settings does not affect the time to

reach a new steady state. However, the modifying this setting does affect the maximum deviation in frequency. Specifically, the deadband is increased from the base case setting of 0.0012 Hz to 0.012 Hz in case 1 and 0.12 Hz in case 2, and the study is repeated. The system frequency response in for cases 1 and 2 is shown in Fig. 15 and Fig. 16, respectively. It is observed that the maximum deviation in frequency increases from 0.64 Hz in the base to 1.35 Hz in case 1 and 1.45 Hz in case 2, respectively. However, there is not much change in the timeframe of primary frequency controls, which is still approximately 30s.

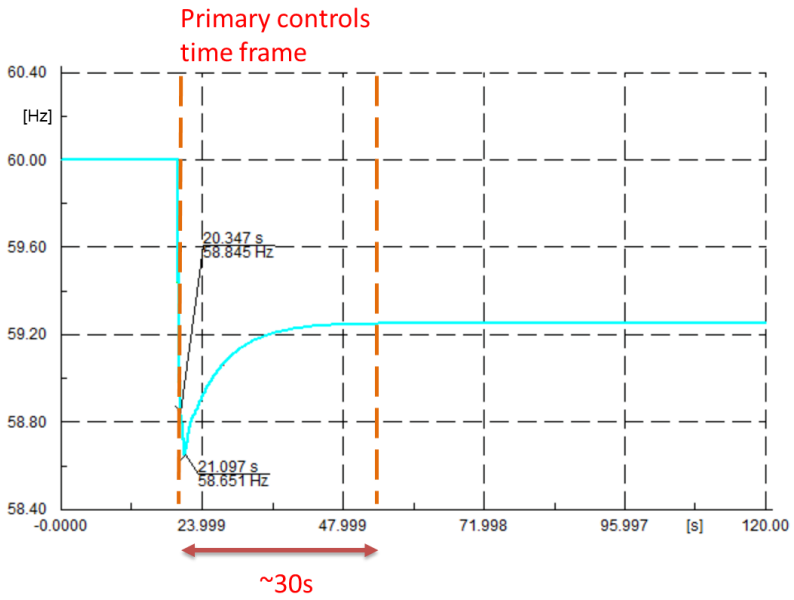

Fig. 15 System frequency response with storage frequency droop setting equal to 0.012 Hz

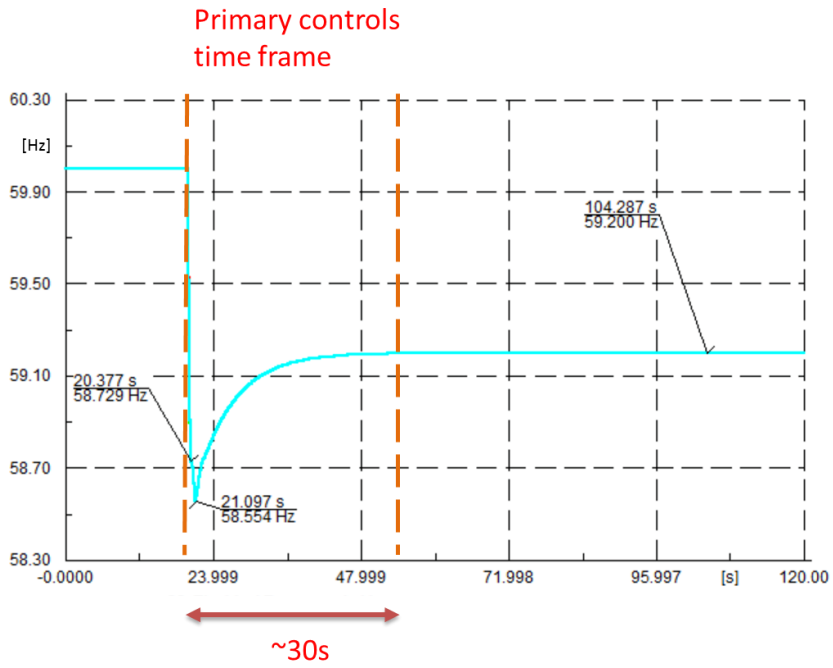

Fig. 16 System frequency response with storage frequency droop setting equal to 0.12 Hz

As discussed in the previous subsection, the optimal time step for the OC strategy was determined to be 10 s. Since the time frame for the primary controls is found to be 30 s, the coupling between dispatching every 10 s and the primary frequency control timeframe needs to be investigated. The total duration of instantaneous frequency limit violations is now introduced to evaluate the impact of time scale coupling. The lower and upper instantaneous frequency limits were selected to be 59.6 and 60.4 Hz based on under and over frequency limits recommended in IEEE 1547 standards [80]. When these frequency limits are violated the relays for under or over frequency protection will be triggered, e.g., load shedding, which is not desirable. It can be seen that dispatching faster but outside the primary control timeframe, (i.e., at least 30

s and less than 5 min) is desirable since the numbers of instantaneous frequency violations were lower as indicated in Table 3.

Table 3 Frequency violation duration with varying time step.

Time step	*Dataset A -Instantaneous Freq. violation duration (s)*	*Dataset B - Instantaneous Freq. violation duration (s)*
10s	293	1003
15s	306	1220
20s	243	1148
30s	192	1136
60s	195	1447
5min	293	N/A
10min	444	N/A

However, dispatching faster but within the primary controls time frame (<30 s), as shown by the 10 s, 15 s and 20 s cases, could lead to an *adverse* frequency performance as indicated by more instantaneous frequency violations. This is related to the adequacy of the power balance constraint. As described in section 2.3.5, two conditions were derived, which ensure the adequacy of the power balance constraint. The first condition implies that the netload forecasts need to be accurate so that the optimal coordination strategy is able to compensate for the variability and uncertainty inherent in netload forecasts. For smaller than 30 s time steps (e.g., 10, 15 and 20 s), this condition held true as discussed in section 3 as indicated by Table 3. However, condition 2 implies that if the dynamics due to disturbances cannot be stabilized within the time

step selected, the power balance constraint may not be an adequate representation of system behavior. So, dispatching faster than 30 s could lead to adverse effects on technical performance because of stronger coupling (poor coordination) with primary frequency controls.

For dataset B, a similar pattern can be seen in Table 3, for the frequency violation duration as the frequency violations are the lowest at 30 s and are sometimes higher at smaller time steps selected within the primary control time frame. Even though 10 s showed the smallest duration of violations, there is no surety that a 10 s time step would not result in adverse frequency impacts based on other netload profiles with different variability characteristics. Since selecting a time step in the primary frequency control time frame could exacerbate frequency performance, it is recommended that the lowest time step outside of the primary control timeframe should be chosen for implementing the OC strategy. This yields the least duration of frequency violations while having a relatively small average number of frequency violations and J_{MAE} as highlighted by Table 1. Therefore, for the microgrid system under study, the time step should be chosen to be 30 s.

4.5.3 Varying prediction horizon

The impact of varying the prediction horizon is studied by fixing the time step to be 30 s. For dataset A, a summary of the technical performance (average frequency violations), economic (J_{MAE}) and computational time is given in Table 4. It can be seen that for prediction horizons larger than 5 min, the economic and technical performance

was not affected as much. For the 30 s prediction horizon case (1 step ahead), the average frequency violations increased to 28% from 8% in the cases with the prediction horizon being larger than 5 min. This is because the storage SOC saturates (i.e., SOC=1), as can be seen from Fig. 17 and that the primary controls of the storage are non-responsive to provide frequency support. Consequently, the system experienced huge frequency excursions as seen from Fig. 18. This indicates a need to ensure that the there is enough look-ahead capability to enable fast acting storage to respond to netload variations with a certain about of forecast error.

There is also an obvious increase in average computational time per step as the prediction horizon increases. However these increases were fairly small. Therefore, the favorable prediction horizon should be 5 or 10 min. According to the SOC profiles shown in Fig. 17, a 10 min prediction horizon may be ideal to ensure the storage is always able to respond to netload disturbances and forecast error. The less conservative prediction horizon is 5 min. For dataset A, there was just look-ahead capability to ensure storage is able to always provide primary frequency response to maintain desirable frequency performance.

Table 4 Summary of technical performance, economics and computational time for dataset A with varying prediction horizon

Prediction Horizon	*Average Freq. Violations (%)*	J_{MAE} *($)*	*Average Computational time per step (s)*
30 s	28.33	6.68	0.004
5 min	8.32	2.69	0.010
10 min	8.49	2.71	0.025
30 min	8.39	2.84	0.139
1 hr	8.87	3.02	0.616

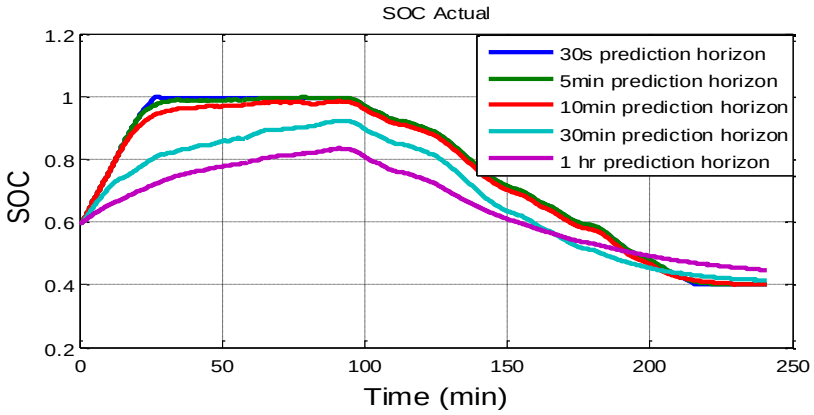

Fig. 17 Actual SOC for each time step considered using dataset A

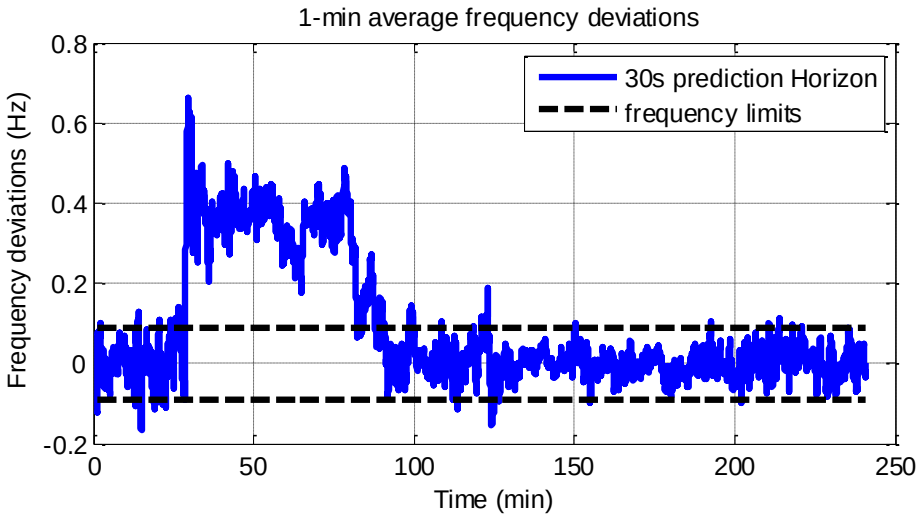

Fig. 18 Moving average frequency deviations for 30s prediction horizon case.

For dataset B, as shown in , the same trend was observed as for dataset A. Specifically, the economic and technical performance was not affected much for prediction horizons that are 5 min or larger. However, for the 30 s prediction horizon case (1 step ahead), results could not be reported since this case resulted in a non-convergence in the dynamic simulation. As mentioned in section 4.5.1, non-convergence in simulation can occur due to a combination of large variations in netload and the battery storage local control settings, which can cause integral windup. In the 30 s prediction horizon case, the changes in battery storage power are less constrained compared to longer prediction horizons because of the temporal SOC limits imposed over the prediction horizon in (17). Therefore, the battery storage setpoints received from the model predictive controller are more volatile. As a result, the simulation for this case failed to converge after sometime.

Table 5, the same trend was observed as for dataset A. Specifically, the economic and technical performance was not affected much for prediction horizons that are 5 min or larger. However, for the 30 s prediction horizon case (1 step ahead), results could not be reported since this case resulted in a non-convergence in the dynamic simulation. As mentioned in section 4.5.1, non-convergence in simulation can occur due to a combination of large variations in netload and the battery storage local control settings, which can cause integral windup. In the 30 s prediction horizon case, the changes in battery storage power are less constrained compared to longer prediction horizons because of the temporal SOC limits imposed over the prediction horizon in (17). Therefore, the battery storage setpoints received from the model predictive controller are more volatile. As a result, the simulation for this case failed to converge after sometime.

Table 5 Summary of technical performance, economics and computational time for dataset B with varying prediction horizon

Prediction Horizon	*Average Freq. Violations (%)*	J_{MAE} *($)*	*Average Computational time per step (s)*
30 s	N/A	N/A	N/A
5 min	19.54	4.05	0.009
10 min	19.65	4.15	0.023
30 min	19.77	4.28	0.142
1 hr	19.84	4.33	0.657

4.6 Summary

This section demonstrates the effectiveness of the proposed OC strategy for an isolated microgrid system containing high penetration of wind generation, as well as, diesel generation and battery energy storage. The performance metrics are discussed in section 4.2. A description of the isolated test system, which is a modified version of the IEEE 123 node test feeder, is given in section 4.3. Since the original IEEE test feeder model did not contain DERs and dump load, models of the additional components included and parameters selected were are further explained. The description of the test cases considered evaluating the performance of the OC strategy is given in section 4.4. Results from studies investigating varying time step and prediction horizon, as well ass, time scale coupling are discussed in section 4.5. The next section discusses general

recommendations on extending the OC strategy design approach to other types of isolated systems with different variability and uncertainty characteristics.

5. RECOMMENDATIONS FOR DESIGNING MULTI-TIME SCALE OC STRATEGIES

5.1 Introduction

The focus of this section is to discuss how the multi-time scale OC strategy proposed in this work can be generalized towards other types of isolated systems. These systems may have different objectives and constraints and different levels of variability and uncertainty based on the diversity in loads and/or non-dispatchable resources. However, for designing or selecting an adequate optimal coordination strategy, the recommendations are given in terms of considerations for the problem formulation (in section 5.2), coordinating with lower level controls (in section 5.3), and forward looking capability (in section 5.4). An example is given, in section 5.5, for developing an OC strategy for an all-electric shipboard power system.

5.2 Formulation considerations

Different types of isolated systems will have different goals. The objectives and constraints should be designed so as to meeting system goals. The formulation proposed in this work is comprehensive for isolated microgrids with a mix of DERs. For systems with a similar mix of DERs, it is easily generalizable. However, thermal limits on lines and cables may be a concern when paths that will be used to supply loads in other systems. If this is a concern, thermal constraints would need to be added with additional network model constraints. Also, in remote isolated systems, one goal may be to manage DERs to meet load demand within fuel supply limits until the next shipment of fuel is

received. Therefore, temporal constraints on fuel supply will need to be reflected in the formulation. Some constraints and objectives chosen could make the problem non-convex, which could lead to obtaining sub-optimal solutions and/or slower computational times. Therefore, a solution method that accommodates a non-convex problem should be selected or an approach to linearize the constraints should be implemented to use an MPC based approach.

5.3 Coordination with lower level control layers

Tertiary controls should be used to make decisions based on regular disturbances that are predictable. When dealing with emergencies in a power system, it is better to implement strategies that rely on local or distributed information and measurements for quick responses to avoid major failures or cause blackouts. If significant disturbances are abrupt and irregular, they can be considered abnormal or emergency events that are not predictable in the short term. Therefore, in a tertiary control problem, proper reserves allocated to compensate for large and abrupt changes. The lower level secondary/primary controls should respond quickly to these irregular disturbances. The time step of the tertiary controller should correspond to the time frame of significant and frequent changes in wind and load. Significant in this case means that the variations in wind and load could threaten the ability to meet the operational performance criteria. As in the type of system discussed in this work, netload variations occur outside of the primary control time frame. However in other types of systems, significant and frequent changes in wind and/or load may occur within the time scale of the lower level controls. If tertiary controls are implemented within time scale of the lower level controls to

match the large variations, this could interfere with control performance in smaller time frames. The following recommendations are given on how to identify which situation is true for a particular system and properly coordinate tertiary controls with lower level controls:

1. Identify non-controllable loads and non-dispatchable generation resources
2. Perform timeframe analysis to determine the primary control time scale. Since the response to disturbances are different based on the mix of resources included and the local control parameters selected, simulations on the dynamical test system representing the system response characteristics are needed.
3. Create several realistic scenarios of variations in non-controllable load and generation in the system of interest. The length of the scenarios can be determined by visually gaging the duration of ramp up/down trends in load and generation profiles with added time to observe behavior following the ramp events.
4. Test a centralized online receding horizon approach on a test system under the realistic scenarios created starting with a typical time step for the tertiary control (e.g., 10 min). The approach should consider a tailored formulation based on system operational goals.
5. Gradually reduce the time step and re-run each scenario until there is overlap with the time scale of the lower level control layer and observe economic performance as well as violations in frequency performance limits. Several cases

could result and are discussed next along with recommendations on selecting the time step for each case:

a. If the average frequency violations persist for all time steps and scenarios considered, as shown in the case 1 example represented in Fig. 19, consider tuning the parameters of the lower layer controls (e.g., proportional control gains selected for generators and storage in the primary controllers). If this does not help resolve the frequency limit violations in the plant, then significant variations due to netload are expected to occur within the time scale of the lower level controls. This means that the chosen DER mix does not have sufficient response capability to maintain frequency performance requirements in the presence of the variability and uncertainty characteristics experienced. Therefore, the frequency performance requirements should be relaxed and/or a new mix of DERs with faster response capability should be considered.

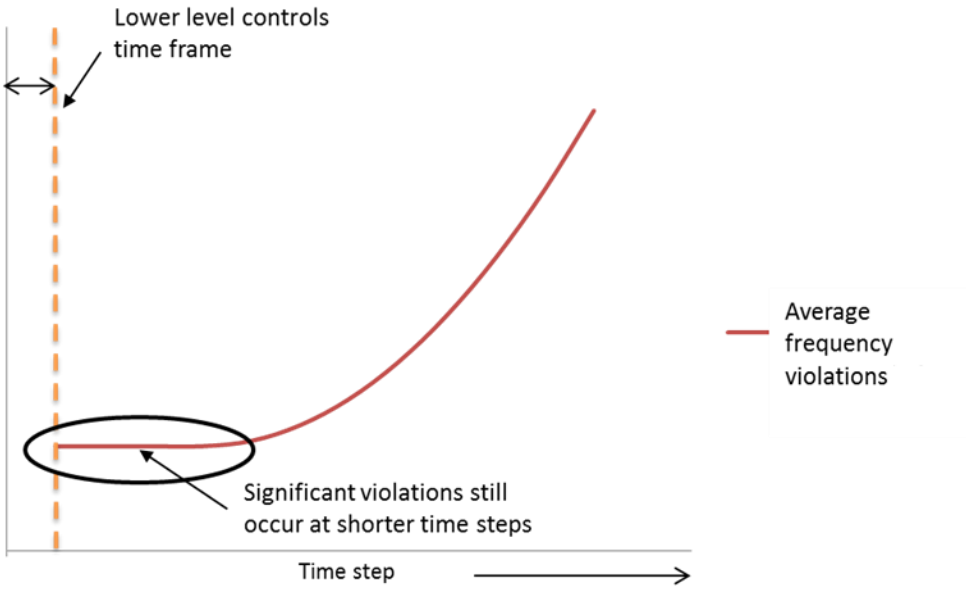

Fig. 19 Case 1 example for time step selection

b. If the number of violations in average frequency performance limits reduces to zero and the trend in economic performance shows continuous improvement as the time step is reduced similar to the example given for case 2 in Fig. 20, then very large variations due to netload changes are expected to occur outside (but close to) lower level control time frame. However, these variations are not great enough to threaten violation of frequency performance limits. In this case, there is potential for improved performance if tertiary controls are dispatched more frequently. However, a reduced time step within the time scale of the lower level controls, as shown in section 4.5.2, could aggravate frequency performance of the lower level controls and cause unnecessary violations if the OC problem

formulation is based on time scale separation principles. This is because steady state constraints based on assumptions of time scale separation (e.g., power balance), which are responsible for meeting operational objectives such as maintaining adequate frequency performance will be rendered invalid. Hence, reducing the time step necessitates including more precise higher order models in the OC formulation that capture system frequency dynamics for better matching of generation and load within the time scale of the lower level controls. Incorporating higher order models could exponentially increase the constraints and decision variables required to solve the receding horizon optimization problem at each time step. Also, the convexity of problem could be affected, resulting in more sub-optimal solutions and/or more computational time needed to make decisions. This increased time may hinder the ability to send optimal setpoint changes when needed using a centralized approach. One solution is to employ high performance computing to speed up the computation time, but the benefits of increasing computational power to include higher order models in the tertiary control formulation should be carefully weighed. Another option is to design a decentralized secondary control approach that relies only on local measurements, similar to the economic AGC approach proposed in [81], to determine control actions in response to large variations and optimize economic performance

However, the recommendation in this case is to choose a time step equivalent to the time frame determined for the lower level controls.

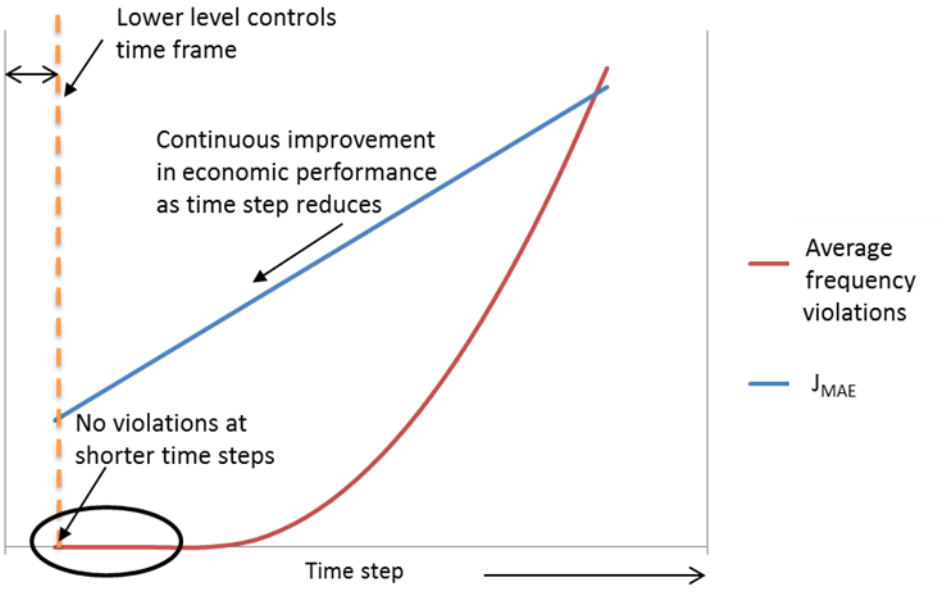

Fig. 20 Case 2 example for time step selection

c. If the number of violations in frequency performance limits reduce to zero and the trend in economic performance shows improvement initially but then becomes constant as the time step reduces, as demonstrated in the example of case 3 in Fig. 21, significant and frequent changes in intermittent resources and/or load are not expected to occur within the time scale of the lower level controls. In this case, time scale separation is a valid assumption; therefore, the static constraints used to maintain

frequency performance are suitable for the OC formulation. Also, the time step chosen for implementing the OC solutions should be selected according to the timeframe of large netload variations. This timeframe will be slower than the time scale of the lower level control layers, so it should not worsen frequency performance. In this case, the largest time step that results in the lowest cost should be selected in this case.

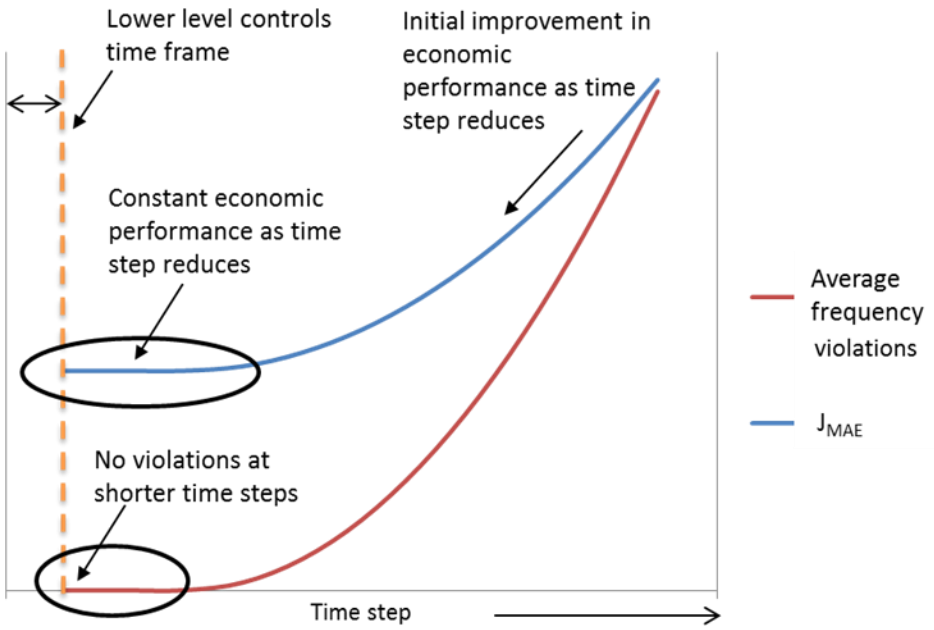

Fig. 21 Case 3 example for time step selection

5.4 Forward looking capability

The prediction horizon of an online approach should be carefully selected to avoid myopic behavior and undue computational burden. If the prediction horizon is too

short, there is a higher probability that temporal constraints will be violated. On the contrary, after a certain time ahead, there will be no additional improvements in OC performance, but the computational time to determine new setpoints would continue to increase. To select the appropriate prediction horizon, the following suggestion is given. Once the time step is selected, re-run test scenarios with the same time step selected and vary the prediction horizon over a specified range. Start with a one-time step ahead prediction horizon and continue to increase until no change or increase is noticed in the most optimal technical performance. In each test, check for saturation or near saturation in temporal limits. If higher levels of variation and uncertainty are expected in the actual system, it may be important to choose a more conservative prediction horizon. Therefore, depending on which prediction horizon resulted in the most optimal technical performance, choose the next highest prediction horizon that does not result in continuous saturation of the temporal constraints.

5.5 Shipboard power system example

A notional all-electric shipboard power system (SPS), studied in [82], is used here as an example to reiterate the points above. SPSs like microgrids have limited capacity and low inertia. The SPSs do not have renewable generation, but some loads are much more variable and abrupt. The loads are categorized in terms of vital, semi-vital and non-vital loads. Some loads have different levels of priority for battle mode and cruiser mode. Many of the vital loads (e.g., pulse weaponry loads and propulsion motors) are typically large relative to individual generation resource committed at any given time.

The formulation should consider semi-vital and vital loads as controllable loads with established priority. Limited fuel constraints will need to be factored in to the problem formulation. In addition, thermal limits for cables could be an issue when dispatching generation, so it may be necessary to consider network constraints in the formulation to make sure an appropriate path is chosen for supplying the loads. High priority propulsion loads will be more predictable based on the speed/power setpoint changes of the ship. Other loads will be predictable based on behavioral patterns or scheduled loads. The generators can be adjusted to follow the propulsion load as the speed of the ship or power setpoint is modulated during cruiser mode. Reserves can be allocated for the high power pulse loads in case the ship switches to battle mode.

Pulse loads, which are given highest priority in battle mode, are very uncertain and happen in the timeframe of 0.1 to 25s [82]. In addition, the magnitude of these loads can range from 20 kW to 70 MW. In cruiser modes, the power rating of high priority propulsion motor loads is 90% of the generation capacity, can ramp to full or no load within 2 s and reach a steady state within 5-15 s. These loads are more predictable yet highly variable in the very short term. Based on the timeframe analysis on the all-electric shipboard presented in [82], the time scale of the lower level controls is 5s. Due to the unpredictability, priority given, and the magnitude of the load pulse and propulsion loads, the OC strategy should ensure proper reserves are available at all times in battle and cruiser mode. With large changes due to pulse and propulsion motor loads occurring so fast within this time frame, 5s should be selected to maintain coordination with lower

level controls and allow the lower level secondary controls to compensate for variations between time steps.

It may be also necessary to predict over longer horizons to ensure the fuel will remain within limits. It is recommended to follow the suggestions given above regarding forward looking capability.

5.6 Summary

This section discusses general recommendations on extending the OC strategy design approach to other types of isolated systems with different variability and uncertainty characteristics. In particular, the additional objectives and constraints for the problem formulation may need to be considered depending on operational goals of an isolated power system, as discussed in section 5.2. Section 5.3 prescribes steps to follow for selecting an appropriate time step and ensuring that the OC strategy is coordinated with lower level primary/secondary controls. Suggestions for selecting a reasonable prediction horizon are given in section 5.4. These recommendations are further discussed in the context of extending the OC strategy to a notional all-electric shipboard power system in section 5.5. The next section discusses conclusions from this work and future work.

6. CONCLUDING REMARKS

6.1 Summary

Isolated power systems with significant variability and uncertainty associated with rapid changes in load and/or renewable generation face many operational challenges with economic and efficient utilization of resources, accelerated resource life degredation, and meeting operational objectives if resources are not coordinated properly. For the OC strategy proposed in this work, the goals were to simultaneously minimize operating costs of diesel generators and maximize the utilization of wind generation, while considering equipment life of DERs, physical limitations on the individual controllable resources and to maintain adequate frequency performance. A comprehensive formulation and robust solution method were presented for optimally coordinating DERs in an isolated power system with high penetration of renewable energy resources. MPC was chosen for the solution method because it is an online receding horizon method that incorporates state feedback and look-ahead capability to compensate for variability and uncertainty.

Another important aspect of this work is the approach used to evaluate the effectiveness of the OC strategy. Because of frequent and significant variations in load and renewables occurring at multiple time scales and the goal of maintaining adequate frequency performance, time scale separation between the OC strategy and the lower level primary controls cannot be assumed. In addition, steady state analysis is not suitable for evaluating the effectiveness of the proposed OC strategy. Therefore, a co-

simulation was setup using DiGSILENT PowerFactory and MATLAB to allow setpoints and feedback measurements to be exchanged between the model predictive controller designed and the isolated power system dynamics at each decision time step. DiGSILENT PowerFactory is an existing power system simulation tool with the capability to studying dynamics. MATLAB was used as the master for initiating and terminating simulations, as well as, modeling the netload disturbance forecaster. In addition, the MATLAB optimization toolbox was used for modeling the model predictive controller behavior. The co-simulation setup enabled the OC analysis to be extended to consider dynamics to understand the impact of the OC strategy on system frequency performance to be investigated.

Since the adequacy of the MPC based OC strategy is dependent on careful selection of time step and the prediction horizon, several scenarios were considered to demonstrate the impact of these parameters on costs, technical performance and computational time. Also time scale coupling was investigated as there were concerns that the coupling between the primary frequency controls and the OC strategy could have adverse effects on frequency performance that cause an increased need for load and generation shedding.

Studies were performed on a simulated isolated microgrid test system modeled using the IEEE 123-node test feeder and realistic wind/load scenarios. For the system under study, a 30 s time step with a 10 min prediction horizon yielded the best performance. The results emphasize the need to dispatch as fast as possible at a time step greater than the primary frequency control time scale to avoid exacerbated frequency

control performance. Also, there is a need to select the prediction horizon to be long enough to avoid saturation of fast acting energy storage, which is critical to maintaining frequency performance in low inertia isolated power networks. In addition, computational time carried little weight in selecting time step and prediction horizon parameters since differences in computational time were negligible in most cases based on the time steps considered and the netload variations and uncertainty in each period.

Results also suggest that the proposed approach is generalizable towards designing multi-time scale optimal coordination strategies for isolated power systems to satisfy both economic and frequency performance. Recommendations are prescribed for extending the OC strategy to other isolated power systems with different characteristics of variability and uncertainty. In particular, recommendations are given regarding considerations for the formulation considerations, coordination with lower level controls and forward looking capability.

6.2 Future work

In this work, it was assumed that active power and frequency are decoupled from reactive power and voltage. The influence of the proposed OC strategy on voltage control performance and reactive power schemes has not been studied. One potential direction for future work is to investigate the impact of the proposed OC strategy on voltage control performance and develop an approach to coordinate with other Volt/VAR management strategies in isolated power systems.

Another direction of future work would be to benchmark the isolated power system dynamic model proposed in this work and make it widely accepted to enable

researchers to test newly developed optimal coordination strategies. Also, developing a standardized set of frequency performance metrics and criteria for isolated microgrids would be immensely valuable in testing the efficacy of new proposed optimal coordination strategies that seek to co-optimize economic and technical performance.

Time step and look-ahead horizon were identified as two key parameters of the OC strategy that affects the economic and system operational performance. In addition, the lower level decentralized controls also have parameters that dominate technical performance, such as droop settings of primary controls. It may also be worthwhile to explore an online adaptive learning-based approach to identify and adjust OC time step and look-ahead horizon, as well as, tune important parameters for lower level controls for varying operating conditions in isolated power systems.

Many research agendas are now giving attention to determining ways to engage demand or flexible loads to accommodate large scale renewable integration into power systems reliably. However, controllability and dependability of demand response are of concern, especially when not employing traditional direct load control. Demand response is dependent by customer preferences, weather conditions, comfort settings and the operating state of the loads, as well as, other drivers. Practical strategies are needed to coordinate a mix of DERs and demand response assets. Extending the OC strategy to consider DR of an aggregated population of end-use loads, which are recognized as good candidates for demand response (e.g., water heaters and air conditioners), is another research path that should be explored.

Finally, the proposed OC strategy is examined in the time scale of operations (seconds to minutes) under normal operating conditions. It would be a very fruitful direction to investigate optimal restoration and black-start strategies in isolated power systems.

REFERENCES

[1] K. L. Butler, N. D. R. Sarma, and V. Ragendra Prasad, "Network reconfiguration for service restoration in shipboard power distribution systems," in *Power Engineering Society Winter Meeting, 2002. IEEE*, 2002, p. 870 vol.2.

[2] K. Davey, "Ship Component in Hull Optimization," *Marine Technology Society Journal*, vol. 39, pp. 39-46, Summer 2005.

[3] G. Gates, D. Shipp, and W. Vilcheck, "Electrical distribution system analysis for off-shore oil production facilities," in *Petroleum and Chemical Industry Conference, 1998. Industry Applications Society 45th Annual*, 1998, pp. 129-137.

[4] B. Kroposki, R. Lasseter, T. Ise, S. Morozumi, S. Papathanassiou, and N. Hatziargyriou. (2008, May-Jun) Making microgrids work. *Ieee Power & Energy Magazine*. 40-53. Available: <Go to ISI>://000258504200010

[5] F. McNamara, "Optimising unit commitment in an island power system," in *Effective Response of a Public Electricity Network to Independent Generators, IEE Colloquium on*, 1993, pp. 8/1-8/7.

[6] L. Qi. (2006). *AC system stability analysis and assessment for Shipboard Power Systems* [Text (Dissertation)]. Available: http://hdl.handle.net/1969.1/3128

[7] W. Wei, W. Daifeng, A. Arapostathis, and K. Davey, "Optimal Power Generation Scheduling of a Shipboard Power System," in *Electric Ship Technologies Symposium, 2007. ESTS '07. IEEE*, 2007, pp. 519-522.

[8] I. Baring-Gould. (2008). *Wind/Diesel Power Systems Basics and Examples*. Available: http://apps1.eere.energy.gov/tribalenergy/pdfs/wind_akwd04_basics.pdf

[9] T. Ackermann, *Wind power in power systems*. Chichester, West Sussex, England; Hoboken, NJ: John Wiley, 2005.

[10] *Abstracts of symposia, invited lectures and free communications*. Bergen: [s.n.], 1973.

[11] M. Milligan, P. Denholm, B. Kirby, K. Porter, E. DeMeo, H. Holttinen, *et al.*, "Wind power myths debunked," *IEEE Power Energ. Mag. IEEE Power and Energy Magazine*, vol. 7, pp. 89-99, 2009.

[12] "IEEE Guide for Design, Operation, and Integration of Distributed Resource Island Systems with Electric Power Systems," *IEEE Std 1547.4-2011*, pp. 1-54, 2011.

[13] T. Burton. (2001). *Wind energy handbook*. Available: http://search.ebscohost.com/login.aspx?direct=true&scope=site&db=nlebk&db=nlabk&AN=78930

[14] A. M. O. Haruni, A. Gargoom, M. E. Haque, and M. Negnevitsky, "Dynamic operation and control of a hybrid wind-diesel stand alone power systems," in *Applied Power Electronics Conference and Exposition (APEC), 2010 Twenty-Fifth Annual IEEE*, 2010, pp. 162-169.

[15] E. P. R. Institute. (April 2011). *Impacts of Wind Generation Integration*. Available: http://www.uwig.org/EPRI-1023166.pdf
[16] R. R. J. Khai D. Le, Jack Feinstein, Henry H. Thompson, H. Matt wolf, Edward C. Stein, A. Daniel Gorski. Jim S. Griffith, "Operational aspects of generation cycling," *Power Systems, IEEE Transactions on*, vol. 5, pp. 1194-1203, 1990.
[17] P. Kundar, J. Paserba, V. Ajjarapu, G. Andersson, A. Bose, C. Canizares, *et al.*, "Definition and classification of power system stability (vol 18, pg 1387, 2004)," *Ieee Transactions on Power Systems*, vol. 19, pp. 2124-2124, Nov 2004.
[18] X. Le, P. M. S. Carvalho, L. A. F. M. Ferreira, L. Juhua, B. H. Krogh, N. Popli, *et al.*, "Wind Integration in Power Systems: Operational Challenges and Possible Solutions," *Proceedings of the IEEE*, vol. 99, pp. 214-232, 2011.
[19] X. Le and M. D. Ilic, "Model predictive dispatch in electric energy systems with intermittent resources," in *Systems, Man and Cybernetics, 2008. SMC 2008. IEEE International Conference on*, 2008, pp. 42-47.
[20] R. Piwko, P. Meibom, H. Holttinen, B. Shi, N. Miller, Y. Chi, *et al.*, "Penetrating insights: Lessons learned from large-scale wind power integration," *IEEE Power Energ. Mag. IEEE Power and Energy Magazine*, vol. 10, pp. 44-52, 2012.
[21] H. Chavez and R. Baldick, "Inertia and Governor Ramp Rate Constrained Economic Dispatch to Assess Primary Frequency Response Adequacy," in *International Conference on Renewable Energies and Power Quality (ICREPQ'12)*, Spain, 2012.
[22] C. L. Chen, T. Y. Lee, and R. M. Jan, "Optimal wind-thermal coordination dispatch in isolated power systems with large integration of wind capacity," *Energy conversion and management.*, vol. 47, pp. 3456-3472, 2006.
[23] C. L. Chen, S. C. Hsieh, T. Y. Lee, and C. L. Lu, "Optimal integration of wind farms to isolated wind-Diesel energy system," *Energy conversion and management.*, vol. 49, pp. 1506-1516, 2008.
[24] C. C. Wu and N. Chen, "Online methodology to determine reasonable spinning reserve requirement for isolated power systems," *IEE proceedings. Generation, transmission, and distribution.*, vol. 150, p. 455, 2003.
[25] D. E. Olivares, A. Mehrizi-Sani, A. H. Etemadi, C. A. Canizares, R. Iravani, M. Kazerani, *et al.*, "Trends in Microgrid Control," *Smart Grid, IEEE Transactions on*, vol. 5, pp. 1905-1919, 2014.
[26] M. Falahi, K. Butler-Purry, and M. Ehsani, "Dynamic Reactive Power Control of Islanded Microgrids," *Power Systems, IEEE Transactions on*, vol. 28, pp. 3649-3657, 2013.
[27] M. Falahi, S. Lotfifard, M. Ehsani, and K. Butler-Purry, "Dynamic Model Predictive-Based Energy Management of DG Integrated Distribution Systems," *Power Delivery, IEEE Transactions on*, vol. 28, pp. 2217-2227, 2013.
[28] N. Hatziargyriou, H. Asano, R. Iravani, and C. Marnay. (2007, Jul-Aug) Microgrids. *IEEE Power & Energy Magazine*. 78-94. Available: <Go to ISI>://000250081400009
[29] J. Driesen and F. Katiraei, "Design for distributed energy resources," *IEEE Power Energ. Mag. IEEE Power and Energy Magazine*, vol. 6, pp. 30-39, 2008.

[30] J. Driesen and F. Katiraei. (2008, May-Jun) Design for distributed energy resources. *IEEE Power & Energy Magazine*. 30-39. Available: <Go to ISI>://000258504200009

[31] R. H. Lasseter, J. H. Eto, B. Schenkman, J. Stevens, H. Vollkommer, D. Klapp, *et al.*, "CERTS Microgrid Laboratory Test Bed," *Power Delivery, IEEE Transactions on*, vol. 26, pp. 325-332, 2011.

[32] C. K. Woo, "What went wrong in California's electricity market?," *Energy*, vol. 26, pp. 747-758, Aug 2001.

[33] N. W. A. Lidula and A. D. Rajapakse, "Microgrids research: A review of experimental microgrids and test systems," *Renewable and Sustainable Energy Reviews*, vol. 15, pp. 186-202, 2011.

[34] E. Alvarez, A. C. Lopez, Go, x, J. mez-Aleixandre, and N. de Abajo, "On-line minimization of running costs, greenhouse gas emissions and the impact of distributed generation using microgrids on the electrical system," in *Sustainable Alternative Energy (SAE), 2009 IEEE PES/IAS Conference on*, 2009, pp. 1-10.

[35] S. Chakraborty, M. G. Simoes, and I. A. S. Ieee Industry Applications Society Annual Meeting, "PV-microgrid operational cost minimization by neural forecasting and heuristic optimization," *Conf Rec IAS Annu Meet Conference Record - IAS Annual Meeting (IEEE Industry Applications Society)*, 2008.

[36] C. M. Colson, M. H. Nehrir, and S. A. Pourmousavi, "Towards real-time microgrid power management using computational intelligence methods," in *Power and Energy Society General Meeting, 2010 IEEE*, 2010, pp. 1-8.

[37] C. M. Colson, M. H. Nehrir, and C. Wang, "Ant colony optimization for microgrid multi-objective power management," in *Power Systems Conference and Exposition, 2009. PSCE '09. IEEE/PES*, 2009, pp. 1-7.

[38] H. Kanchev, D. Lu, B. Francois, and V. Lazarov, "Smart monitoring of a microgrid including gas turbines and a dispatched PV-based active generator for energy management and emissions reduction," in *Innovative Smart Grid Technologies Conference Europe (ISGT Europe), 2010 IEEE PES*, 2010, pp. 1-8.

[39] H. Vahedi, R. Noroozian, and S. H. Hosseini, "Optimal management of MicroGrid using differential evolution approach," in *Energy Market (EEM), 2010 7th International Conference on the European*, 2010, pp. 1-6.

[40] D. E. Olivares, C. A. Canizares, M. Kazerani, I. P. G. M. T. E. o. Transportation, and F. the Grid of the, "A centralized optimal energy management system for microgrids," *IEEE Power Energy Soc. Gen. Meet. IEEE Power and Energy Society General Meeting*, 2011.

[41] N. Hatziargyriou, G. Contaxis, M. Matos, J. A. P. Lopes, G. Kariniotakis, D. Mayer, *et al.*, "Energy management and control of island power systems with increased penetration from renewable sources," in *Power Engineering Society Winter Meeting, 2002. IEEE*, 2002, pp. 335-339 vol.1.

[42] A. Seon-Ju and M. Seung-Il, "Economic scheduling of distributed generators in a microgrid considering various constraints," in *Power & Energy Society General Meeting, 2009. PES '09. IEEE*, 2009, pp. 1-6.

[43] N. Sieber, "Chow, J. H. (ed.), Time-Scale Modeling of Dynamic Networks with Applications to Power Systems. Berlin-Heidelberg-New York, Springer-Verlag 1982. IX, 218 S. DM 28,50. US $ 11.40. ISBN 3-540-12106-4 (Lecture Notes in Control and Information Sciences 46)," *ZAMM - Journal of Applied Mathematics and Mechanics / Zeitschrift für Angewandte Mathematik und Mechanik*, vol. 64, pp. 340-340, 1984.

[44] X. Xia and A. M. Elaiw, "Optimal dynamic economic dispatch of generation: A review," *Electric Power Systems Research*, vol. 80, pp. 975-986, 2010.

[45] *Diesel Service and Supply Data Sheet*. Available: http://www.dieselserviceandsupply.com/temp/Fuel_Consumption_Chart.pdf.

[46] *Wind Induced Coal Plant Cycling Costs and the Implications of Wind Curtailment for Public Service Company of Colorado*. Available: http://www.uwig.org/11M-710E_WindInducedCoalPlantCycling.pdf

[47] G. Delille, Franc, x, B. ois, and G. Malarange, "Dynamic frequency control support: A virtual inertia provided by distributed energy storage to isolated power systems," in *Innovative Smart Grid Technologies Conference Europe (ISGT Europe), 2010 IEEE PES*, 2010, pp. 1-8.

[48] C. Abbey and G. Joos, "Sizing and power management strategies for battery storage integration into wind-diesel systems," in *Industrial Electronics, 2008. IECON 2008. 34th Annual Conference of IEEE*, 2008, pp. 3376-3381.

[49] A. Parisio and L. Glielmo, "Energy efficient microgrid management using Model Predictive Control," in *Decision and Control and European Control Conference (CDC-ECC), 2011 50th IEEE Conference on*, 2011, pp. 5449-5454.

[50] L. Xiaoping, D. Ming, H. Jianghong, H. Pingping, and P. Yali, "Dynamic economic dispatch for microgrids including battery energy storage," in *Power Electronics for Distributed Generation Systems (PEDG), 2010 2nd IEEE International Symposium on*, 2010, pp. 914-917.

[51] M. Chen and G. A. Rincon-Mora, "Accurate Electrical Battery Model Capable of Predicting Runtime and I-V Performance," *IEEE TRANSACTIONS ON ENERGY CONVERSION EC*, vol. 21, pp. 504-511, 2006.

[52] A. R. Bergen and V. Vittal, *Power systems analysis*. Upper Saddle River, NJ: Prentice Hall, 2000.

[53] A. S. Debs, *Modern power systems control and operation*. Boston: Kluwer Academic Publishers, 1988.

[54] J. A. Momoh, *Electric power system applications of optimization*. Boca Raton: CRC Press, 2009.

[55] J. A. Momoh, "Optimal Methods for Power System Operation and Management," in *Power Systems Conference and Exposition, 2006. PSCE '06. 2006 IEEE PES*, 2006, pp. 179-187.

[56] M. D. Ilic and J. Zaborszky, *Dynamics and control of large electric power systems*. New York: Wiley, 2000.

[57] E. F. Camacho and C. Bordons, *Model predictive control*. Berlin; New York: Springer, 1999.

[58] J. H. Lee, "Model predictive control and dynamic programming," *Int. Conf. Control, Autom. Syst. International Conference on Control, Automation and Systems*, pp. 1807-1809, 2011.
[59] J. A. Momoh and Z. Yi, "Unit commitment using adaptive dynamic programming," in *Proceedings of the 13th International Conference on Intelligent Systems Application to Power Systems*, 2005, p. 4 pp.
[60] W. B. Powell, *Approximate dynamic programming : solving the curses of dimensionality*. Hoboken, N.J.: Wiley-Interscience, 2007.
[61] F. Y. Wang, D. Liu, and H. Zhang, "Adaptive dynamic programming: An introduction," *IEEE Computational Intelligence Magazine*, vol. 4, pp. 39-47, 2009.
[62] *DIgSILENT PowerFactory*. Available: <http://www.digsilent.de/Software/DIgSILENT_PowerFactory/>
[63] *PSCAD*. Available: https://hvdc.ca/pscad/
[64] *Power System Toolbox*. Available: http://www.eps.ee.kth.se/personal/vanfretti/pst/Power_System_Toolbox_Webpage/PST.html
[65] *PSSE*. Available: http://w3.siemens.com/smartgrid/global/en/products-systems-solutions/software-solutions/planning-data-management-software/planning-simulation/pages/pss-e.aspx
[66] *BAL-001-2 - Real Power Balancing Control Performance Standard Background Document*. Available: http://www.nerc.com/pa/Stand/Project%202010141%20%20Phase%201%20of%20Balancing%20Authority%20Re/BAL-001-2_Background_Document_Clean-20130301.pdf
[67] *IEEE PES Distribution Test Feeders*. Available: <http://www.ewh.ieee.org/soc/pes/dsacom/testfeeders/index.html>
[68] DIgSILENT, "Technical documentation: Synchronous generator," 2010.
[69] *Marelli Generators: Data Sheets Three phase Synchronous Generators*. Available: http://www.powertechengines.com/MarelliData/Data%20Sheet/COMM.DSG.001.6%20GB.pdf
[70] P. T. Inc., "PSS/E-28 Program Operations Manual," November 2001.
[71] P. T. Inc., "Program Application Guide," November 2001.
[72] DIgSILENT, "Application Manual: Simulation of a BESS with Power Factory," March 2010.
[73] *Exergonix battery energy storage datasheet*. Available: http://www.exergonix.com/documents/BESS_brochure.pdf
[74] A. Hansen, F. Iov, P. Sørensen, N. Cutululis, C. Jauch, and F. Blaabjerg. (2003). *Dynamic wind turbine models in power system simulation tool DIgSILENT*. Available: http://www.digsilent.es/tl_files/digsilent/files/powerfactory/application-examples/ris-r-1400.pdf
[75] DIgSILENT, "Generic model description: DFIG template," September, 2011.

[76] *Vestas V47 datasheet*. Available: http://www.google.com/url?sa=t&rct=j&q=vestas%20v47&source=web&cd=2&sqi=2&ved=0CDcQFjAB&url=http%3A%2F%2Fwww.iufmrese.cict.fr%2Fconcours%2F2002%2FCG_2002STI_lycee%2FPour_en_savoir_plus%2FVestas_V47.pdf&ei=ie_pUIqCFcjL0AGz9IHgDw&usg=AFQjCNGu_ohCTb0dbDZvdaD0meoyMjaIxQ

[77] *GridLAB-D 2014*. Available: http://www.gridlabd.org

[78] *GridLAB-D Residential Module User's Guide*. Available: http://sourceforge.net/apps/mediawiki/gridlab-d/index.php?title=Residential_module_user%27s_guide

[79] J. C. Fuller, N. Prakash Kumar, C. A. Bonebrake, and R. W. A. Pacific Northwest National Laboratory, "Evaluation of Representative Smart Grid Investment Project Technologies: Demand Response," United States PNNL-20772, 2012.

[80] "IEEE Standard for Interconnecting Distributed Resources with Electric Power Systems - Amendment 1," *IEEE Std 1547a-2014 (Amendment to IEEE Std 1547-2003)*, pp. 1-16, 2014.

[81] L. Na, C. Lijun, Z. Changhong, and S. H. Low, "Connecting automatic generation control and economic dispatch from an optimization view," in *American Control Conference (ACC), 2014*, 2014, pp. 735-740.

[82] X. Feng, "A bio-inspired multi-agent system framework for real-time load management in all-electric ship power systems," Texas A&M University, College Station, Tex., 2012.